THE PENNSYLVANIA STATE UNIVERSITY
SCHREYER HONORS COLLEGE

DEPARTMENT OF BIOLOGY

GENETIC AND BIOCHEMICAL ANALYSIS OF THE FUNCTIONS OF STARCH BRANCHING ENYMES IN *Zea mays.*

JENNIFER BLACKMAN
Spring 2010

A thesis
submitted in partial fulfillment
of the requirements
for a baccalaureate degree
in Biochemistry and Molecular Biology
with honors in Biology

Reviewed and approved* by the following:

Mark Guiltinan
Professor of Plant Molecular Biology
Thesis Supervisor

Daniel Cosgrove
Professor of Biology
Honors Adviser

* Signatures are on file in the Schreyer Honors College.

ABSTRACT

Zea mays L. (maize) contains starch branching enzymes (SBEs), which are glycosyl transferases that determine the structure of the starch within the plant by adding branches to amylose to form amylopectin. There are three forms of starch branching enzymes, SBEI, SBEIIa, and SBEIIb. Since *Sbe2a* and *Ae (Sbe2b)* are expressed both in the kernel endosperm and within mature pollen, these are thought to play specific roles in the synthesis of starch during plant development. Although the role of SBE has been well characterized in maize endosperm, the role of these genes in the other parts of the plant such as leaves and pollen is less well studied. To examine the role of SBEs in maize, two main approaches were taken. In the first chapter of the thesis, the proteins were studied *in vivo* through the use of a reverse genetics approach. In the second chapter of the thesis, purified SBE proteins were prepared to investigate *in vitro* the regulation of their biochemical activities. To assess the role(s) of SBEs in pollen development and successful pollination, we first determined the frequency of genetic transmission of the *sbe2a-Mu* mutation, a knock out allele generated by a *Mutator* transposon insertion (herein referred to as *sbe2a-Mu*), and *ae* alleles in an outcross of *Sbe2a/sbe2a-Mu; ae/ae* pollen to a plant wildtype for *Sbe2a* and *Ae*. In contrast to the expectation that 50% of offspring should contain the *sbe2a-Mu* allele, only 9% transmission of the allele was observed in the *ae* background. This suggests that pollen germination and/or growth requires the function of at least one of the SBEII class genes for proper function. Secondly, we tested the *sbe2a-Mu; ae* double mutant's effect on pollen tube germination and/or growth. To address this, the lengths of double mutant pollen tubes were compared to single *ae* mutant tubes growing within wildtype silks and on synthetic media plates. *In vitro*, the lengths of the *sbe2a-Mu; ae* double mutant

pollen tubes were shorter than *ae* single mutant types. Observations of pollen germination and growth made *in vivo* were consistent with this result. Fewer of the *sbe2a-Mu; ae* double mutant tubes were observed within wildtype pollinated silks as compared to the *ae* single mutant pollen. Together, these results indicate that the decrease in transmission rate of the *sbe2a-Mu* and *ae* mutant alleles to progeny could be due to the inability of the double mutant pollen to either germinate or grow as fast as the *ae* single mutant or wild type pollen. It is likely that the slow rate of growth observed in *sbe2a-Mu; ae* double mutant pollen results in its low rate of pollination and allele transmission. This suggested the hypothesis that wildtype and *sbe* single mutants are able to out-compete the *sbe2a-Mu; ae* double mutant pollen grains and successfully pollinate egg cells at a significantly higher rate. As part of a study of the biochemical regulation of the SBE enzymes, recombinantly expressed starch branching enzymes were expressed in *E. coli*, purified and their biochemical activities examined to investigate their regulation by redox conditions. Mutants were obtained with both single and multiple mutations in order to study the possible residues that are pertinent to redox regulation of these enzymes.

TABLE OF CONTENTS

LIST OF FIGURES

LIST OF TABLES

ACKNOWLEDGEMENTS

I would first like to thank Dr. Mark Guiltinan, my advisor, for his guidance both through my research and the writing of this document. I also want to extend a special thank you to Dr. Marna Yandeau-Nelson, who helped me through all of the research involved in this thesis as well as spent great amounts of time helping me to edit the writing. I want to thank Dr. Siela Maximova for her support through the writing process and in aspects of the research. I want to also thank Ann Young and Sharon Pishak, for their guidance and friendship though the years working with them. Finally, I would like to thank my family for their support through the thesis writing process.

Chapter 1

Transmission of *sbe2a-Mu; ae* Double Mutant

Introduction

Starch and Starch Biosynthesis

Starch is a polysaccharide that allows for the storage of excess glucose in plants. There are two main components of starch: amylose, which is composed of linear chains of α-(1,4) linked glucose units, and amylopectin, which is a branched glucan polymer (Figure 1, adapted from 1). Whereas amylose is primarily linear, 5% of the linkages within amylopectin are α-(1,6), which

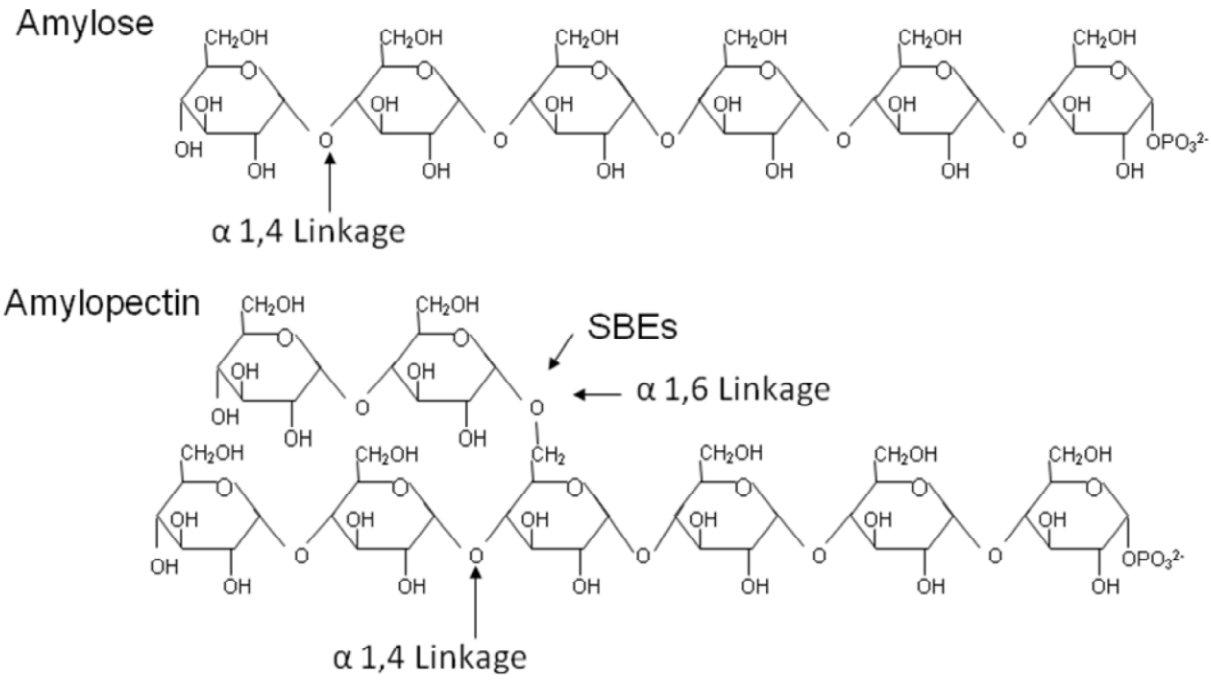

Figure 1: Structures of Amylose and Amylopectin
The structure for amlyose and amylopectin, displaying the differing linkages between glucose molecules. In amylose, glucose monomers are connected by α-(1,4) linkages, generating linear chains. Amylopectin has α-(1,4) linkages as well as α-(1,6) linkages catalyzed by starch branching enzymes, which introduce branches into the molecule.

introduce branches into the structure (reviewed in James *et al.*, 2003). The relative ratio of amylopectin to amylose varies according to the plant tissue and species. For example, in maize, endosperm starch is composed of 70% amylopectin and 30% amylose, whereas starch in the leaf is composed of 85% amylopectin (33, 34, 35). In pollen, 80% of the starch is amylopectin and 20% is amylose (20).

Starch serves different purposes across different plant organs (e.g., kernel endosperm, leaves and pollen). Within the kernel, endosperm starch serves as long-term energy storage and is utilized during germination of the kernel embryo (4). In contrast, starch synthesized within the leaf is transitory: starch accumulates during photosynthesis and at night is degraded to serve as a major source of energy throughout the plant. Starch synthesis within pollen occurs during the final stages of pollen maturation and is critical to pollen survival (4). Starch serves as a reserve source of energy for pollen germination and also a checkpoint of pollen maturity. In fact, when there are low levels of starch, pollen maturation can be terminated in maize (4).

Starch synthesis is initiated by ADP-glucose pyrophosphorylase, which converts glucose into ADP-glucose (1). Subsequently, three additional classes of enzymes are required for starch synthesis. Starch synthase elongates the starch molecule by forming α-(1,4) linkages between ADP-glucose monomers and the growing glucan chain (1). Starch branching enzymes (SBEs) are glycosyl transferases, which act on the glucan chain to generate α-(1,6) linkages and thereby introduce branches into the molecule, which will be described in more detail below (1). Debranching enzymes (DBEs) are used both in starch formation as well as in degradation. There are two forms of starch debranching enzymes, isoamylase-type and pullulanase-type (7). Both function in glucan hydrolysis by hydrolyzing α-(1,6) linkages during kernel starch formation and degradation and have unique functions in carbohydrate synthesis, storage and utilization (7).

The loss or reduction of these debranching enzymes results in phytoglycogen production (a highly branched starch-related molecule resembling animal glycogen found in large quantities in the water soluble polysaccharide fraction of endosperm (28) at the expense of amylopectin synthesis (26)). Thus, both types of starch debranching enzymes are therefore required during starch synthesis and are involved in the construction of amylopectin fine structure (26).

Starch Synthesis in Pollen

Pollen exists as grains, which upon landing on the silks of a maize ear shoot, germinate and generate pollen tubes, which grow through the silk to pollinate egg cells. Various factors affect the rate at which pollen tubes grow through silks (10). These factors include the arrangement of organelles within the pollen, concentrations of calcium and hydrogen ions, the functions of signaling molecules, and the macromolecules within the pollen (10). Pollen tube growth is rapid and highly polarized, with the growth occurring at the tip or the apex of the tube. Secretory vesicles located inside the pollen tube transport the cellular building blocks that are required for growth to the apex (10). At the apex, these building blocks are incorporated into the extending pollen tube by exocytosis. This process is extremely efficient, sometimes supporting growth at a rate of up to 1 centimeter per hour in maize (10).

The manner in which the pollen tubes grow is dependent on the amount of starch that is stored in the pollen grain (13). Starch serves as an energy source for pollen germination and its accumulation serves as a checkpoint for pollen maturity in maize (13). Mature pollen grains in different plant species have different amounts of starch depending on the type of pollination (i.e., abiotic versus biotic), length of the path the pollen must travel, and its phylogenetic classification (11).

The starch present in pollen grains is critical to normal pollen function. For example, it has been demonstrated in maize that a lack of starch is linked to pollen sterility (13). Fertile pollen grains contain starch whereas sterile pollen does not (13). Pollen maturation in maize is prematurely terminated if starch levels remain lower than a threshold point after the starch accumulation phase of development and the plant is rendered sterile (13). For example, in maize exhibiting S-type cytoplasmic male sterility, pollen collapses during the starch accumulation phase of development (13).

In contrast, it has recently been shown in tomato that male sterility is associated with an accumulation of starch in the mature pollen grains (11). The negative effects of starch accumulation were demonstrated in tomato mutants containing non-functional α-glucan water dikinase, an enzyme that controls phosphate content in starch. Mutation of this enzyme leads to a decrease in starch phosphate levels and a reduction in starch degradation, causing excess starch accumulation within pollen (11). This excess in starch has mechanical and metabolic consequences, in that the mutant pollen contains very large starch granules in its plastids and the pollen has reduced levels of sugar, respectively (11). This suggests that in tomato a normal level of starch is important for fertility. The different responses to starch accumulation in tomato and maize may possibly be due to the length to which the pollen tubes must grow. Pollen tubes grow longer distances in maize, which has very long silks, and therefore more starch may be required for pollen viability and pollen tube growth in maize as compared to tomato.

Little is known about the starch biosynthesis pathway in pollen (13). However, research has shown that some enzymes involved in starch synthesis in pollen are expressed at different levels as compared to other tissues of the plant. ADP glucose phosphorylase (AGPase) is an active enzyme in pollen starch biosynthesis with activity levels lower than observed in

endosperm extracts (20). However, UDP glucose phosphorylase, which is active in pollen and endosperm, is three times more active in pollen than endosperm (20). The *hexose transporter*, *PM H^+-ATPase*, and *Grf1* genes (13) are also upregulated during starch synthesis in pollen. The hexose transporter provides energy for pollen germination and pollen tube growth (23). The *PM H^+-ATPase* plays a role in pH homeostasis, and when mutated, male fertility is affected (24). *Grf1* genes encode general regulatory factors that regulate the process of starch biosynthesis (25). In pollen there is greatly increased activity of invertase (20), which cleaves sucrose to hexose sugars to start starch biosynthesis (13). In addition to invertase, *Sus1*-encoded Suc synthase (SuSy), which plays a role in energy metabolism and carbon allocation, is an important enzyme (22, 13) during starch biosynthesis (13). Both invertase and SuSy play a role in carbon partitioning and sugar sensing (22). However, SuSy has only a minor role in pollen grains starch biosynthesis (13). Interestingly, there are several additional genes involved in starch biosynthesis that do not function in pollen, including sucrose synthetase, hexokinase, the P-glucomutases, and glucose-P isomerase (20). Together, this enzymatic data suggests that there may be different mechanisms of starch synthesis in pollen versus other tissues of the plant.

Starch Branching Enzymes (SBEs)

Starch Branching Enzymes (SBEs) play an important role in starch synthesis. Specifically, this enzyme class facilitates the branching reaction in the amylopectin fraction of starch. This glucosyltransferase works by hydrolyzing an α-(1,4) linear linkage in a glucan chain and reattaching the chain by forming an α-(1,6) bond (2, 6; Figure 2, adapted from 1) and introducing a branch.

There are two classes of SBEs in maize: Class I includes the SBEI enzyme isoform and Class II includes both the SBEIIa and SBEIIb isoforms (6). Functionally, SBEI tends to produce longer constituent chains than SBEII (2,8). In Class II, SBEIIb is encoded by the *amylose extender* gene (*ae*), which is a homolog of *rugosus* (*r)* in pea, which was famously used by Mendel in his study of the law of inheritance (29). The *rugosus* mutant results in a wrinkled seed (30, 31). Likewise, in the absence of SBEIIb maize kernel starch exhibits much less branching and the kernel crown appears shriveled or wrinkled (5). The other Class II SBE, SBEIIa, is encoded by *sbe2a* and is very important in starch synthesis in the leaf. In the absence of SBEIIa in a mutant plant created by a *Mutator* transposon insertion (designated as *sbe2a-Mu*) kernel starch is unaffected, but in the leaf there is even less branching than is observed in *ae*

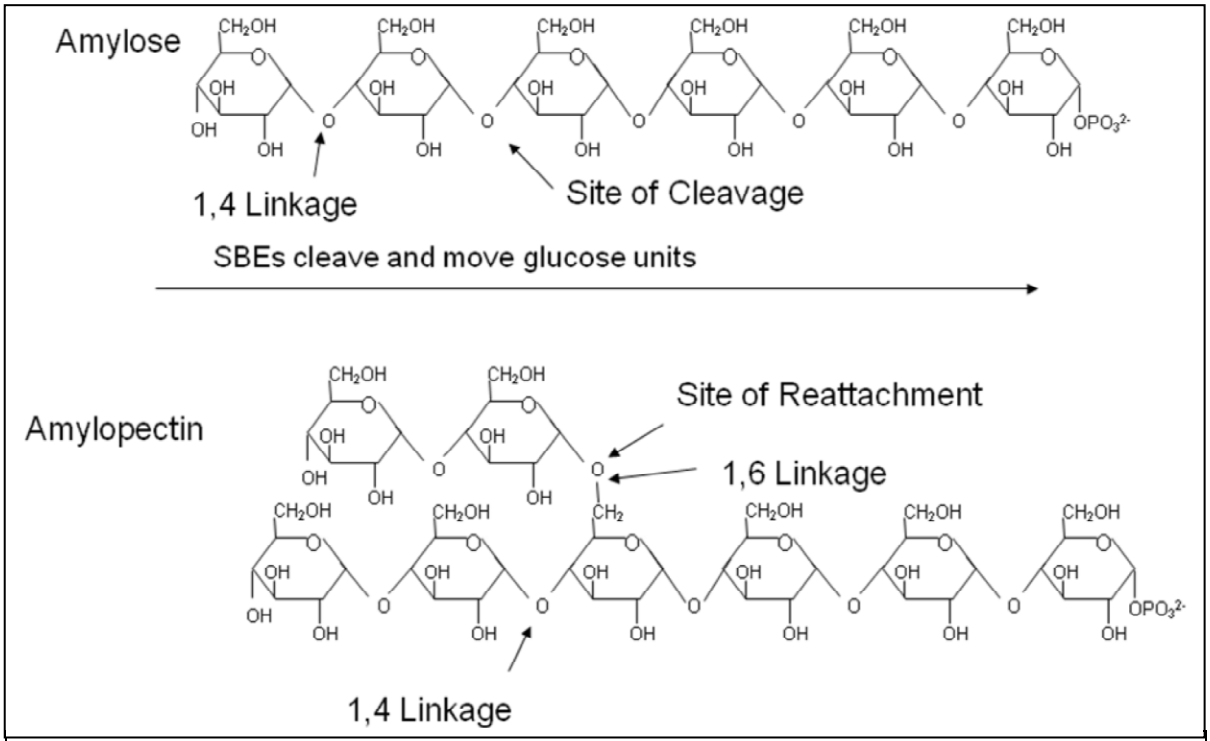

Figure 2: Branching Reaction Facilitated By SBE
Conversion of amylose to amylopectin by starch branching enzymes, which facilitate the movement of some glucose units from an α -(1,4) linkage to an α –(1,6) linkage, creating branches in the starch structure.

endosperm starch and severe premature leaf senescence is observed (5). Whereas the removal of either Class II enzyme yields a visible phenotype within a specific plant organ, plants lacking functional SBEI (*sbe1-Mu* mutants created by a *Mutator* transposon insertion) show no visible phenotypic changes compared to wildtype (5). However, the *sbe1-Mu* mutation has an observable effect on amylopectin structure when SBEIIb is not functional (i.e., in an *ae* mutant) (5). The double mutant *sbe1-Mu*; *ae*, when present in combination with the *wx* mutant, which contains a non-functional granule-bound starch synthase and does not produce amylose, exhibits an intermediate amount of amylopectin. The amylopectin has less branching compared to *wx*, but more compared to *ae; wx*, which is different from either single mutant *sbe1-Mu* or *ae* endosperm starch (5).

While *sbe1-Mu; sbe2a-Mu* and *sbe1-Mu; ae* double mutants are easily generated by genetic crossing and identifiable by genotyping, it is interesting that it is difficult to recover progeny for which both Class II enzymes are mutated (the *sbe2a-Mu; ae* double mutant; summarized in Table 1). This observation was the basis for the research that is the central part of this thesis. The following pages therefore focus on understanding the reason for the difficulty in recovering the progeny with both Class II enzymes mutated.

Table 1: Phenotypes for SBE mutants

Genotype	Leaf Phenotype	Kernel Phenotype	Leaf Starch Structure	Endosperm Starch Structure (branching)
sbe1-Mu	Normal	Normal	Normal	Normal
sbe2a-Mu	Premature senescence	Normal	Chains primarily linear, little or no branching	Normal
ae	Normal	Dark, small, wrinkled	Normal	Less branching compared to wildtype (higher amylose and amylopectin with longer CL); in *wx*, less branching
sbe1-Mu; sbe2a-Mu	Premature senescence	Normal	ND	Normal
Sbe1-Mu; ae	Normal	*ae* phenotype ; darker kernels	ND	In *wx*, amylopectin with less branching (longer CL) compared to *wx*; but more branching compared to *ae wx*
sbe2a-Mu; ae	Premature senescence	Identical to *ae*; Present in only 1% of seed	Similar to *sbe2a-Mu*	*ae*<*sbe2a-Mu; ae* (higher amylose and amylopectin with longer CL) < wildtype branching
sbe1-Mu; sbe2a-Mu; ae		No kernels identified		

Thesis Rationale and Organization

To understand the impact of *sbe* mutant combinations on endosperm starch, Dr. Yuan Yao, a former member of Dr. Guiltinan's laboratory at The Pennsylvania State University, strived to obtain the SBE Class II double mutant, *sbe2a-Mu; ae*, by selfing a *Sbe2a/sbe2a-Mu*; *ae/ae* plant. According to Mendelian genetics, one would expect that 25% of resulting progeny would be *sbe2a-Mu/sbe2a-Mu; ae/ae* double mutants. Interestingly, only ~1% of progeny were *sbe2a-Mu; ae* double mutants. Dr. Marna Yandeau-Nelson and Ryan Wolff later repeated this study in a

larger scope within Dr. Guiltinan's laboratory, *Sbe2a/sbe2a-Mu; ae/ae* plants were selfed and the progeny were planted in large numbers (700-800 kernels). A similar low recovery was observed, only 6.4% of the progeny were double mutant for the Class II SBEs.

Because both Class II enzymes are expressed within the kernel endosperm and pollen, two hypotheses were developed. First, the low recovery of *sbe2a-Mu; ae* double mutants could be due to the failure of the majority of *sbe2a-Mu; ae* kernels to germinate. This could be due to a requirement that at least one of the Class II SBEs must be functioning in the kernel endosperm to produce a starch structure that is digestable by the germinating embryo. This is a reasonable hypothesis because *Sbe2a* and *Ae* are expressed in the kernel endosperm and may be necessary to produce a digestible starch structure (27). However, our data does not support this hypothesis. The *sbe2a-Mu; ae* double mutant was only recovered at a rate of 6.4% versus the expected rate of 25%. Therefore, there was 18.6% reduction in expected *sbe2a-Mu; ae* double mutants. If these *sbe2a-Mu; ae* double mutants kernels were present but had failed to germinate, we would expect the germination rate to be 100% - 18.6% (i.e., double mutant kernels) = 81.4%. Instead, germination rates were almost always above 95% from progeny of a selfed *Sbe2a/sbe2a-Mu; ae/ae* plant, which is similar to normal wildtype, non-mutant maize. The few kernels that did not germinate were genotyped and shown not to be double mutant. This hypothesis is therefore not well supported by the evidence, since we were able to recover double mutant seeds and seedlings, though at a lower frequency than expected. Furthermore, the double mutant seed germinated at normal frequencies and the resulting seedlings had normal growth rates. Taken together, this data demonstrates that the reduced recovery of the *sbe2a-Mu; ae* double mutant was not due to a lower rate of seed germination or a kernel defect, but instead the double mutant kernels were not being generated at the rate expected.

Alternatively, we hypothesized that the lack of both Class II SBEs could affect pollen function. *Sbe2a* and *Ae (Sbe2b)* gene products could function together within the pollen such that at least one of the Class II enzymes must be present to yield starch quantity and/or quality necessary for pollen tube germination and/or growth. Results by Huan Xia in our lab had recently demonstrated that the double mutant *sbe2a; ae* starch from endosperm is more slowly degraded by enzymatic digestion then normal starch (38). If this observation were to also be true for pollen starch degradation rates, this would suggest the possibility that pollen tubes would not be able to obtain sufficient energy flux from digesting starch during pollen tube growth to support normal rates of tip growth (38). The goal of this project is to address this hypothesis and determine if pollen development is affected in the absence of both SBEIIa and SBEIIb.

This project consisted of two parts. The goal of the first part was to determine the rate that the *sbe2a-Mu* and *ae* alleles are transmitted together in an outcross of pollen from a *Sbe2a/sbe2a-Mu; ae/ae* plant crossed to the ear shoot of a plant wildtype for *Sbe2a* and *Ae*. This cross directly tests whether there is a pollen defect in the absence of any potential defects in egg cells lacking *sbe2a-Mu* and *ae.* Large numbers of progeny were grown and genotyped for the presence of either the *Sbe2a* or *sbe2a-Mu* alleles (See Methods). The second goal was to assess whether pollen tube growth is affected in *sbe2a-Mu; ae* double mutant pollen, by comparing pollen viability and the length of double mutant pollen tubes to *Sbe2a*; *ae* pollen tubes.

If the hypothesis that pollen tube germination or growth is affected in the double mutant is correct, we would expect that the double mutant pollen tubes will be fewer, or shorter than the wildtype pollen tubes.

Materials and Methods

Genetic Stocks

Starch branching enzyme mutants were identified, isolated, and analyzed previously in the Guiltinan laboratory (2, 35). The *sbe2a-Mu* mutants were found to show reduced branching in the leaf, endosperm, and kernel starch and a visible phenotype that resembled accelerated senescence (35). In *sbe1-Mu* mutants, the starch structure in both the endosperm and the leaves is indistinguishable in comparison to wildtype plants (2). The *ae* mutant shows decreased branching of the starch (5). These identified class II mutants were used in this study. In the summer of 2007, *Sbe2a/sbe2a-Mu* heterozygotes in an *ae/ae* homozygous mutant background were both selfed and crossed to *Sbe2a; Ae* wildtype or *Sbe2a*; *ae* single mutant genetic stocks.

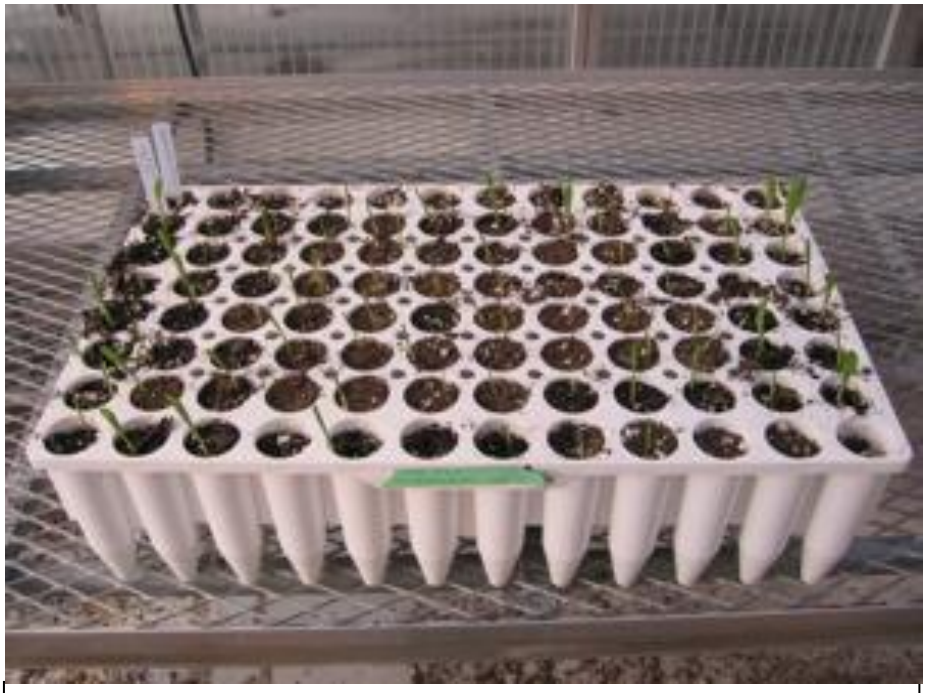

Figure 3: High-throughput Growth of Maize Plants.
Kernels were germinated in 96-well flats and were grown for 1-2 weeks prior to tissue sampling for DNA extraction and PCR genotyping.

Progeny from these crosses were germinated and genotyped for *sbe2a-Mu* and *ae* alleles using PCR reactions as described below. Confirmed *sbe2a-Mu; ae* homozygous double mutant plants were transplanted to the field at Penn State Horticulture Farm (Rock Springs, Pa) and the greenhouse of 4th level Life Science Building in the summer of 2008.

DNA Isolation

Ears were harvested and dried, and kernels were shelled from the ears. Kernels were then germinated in 96-well flats (Figure 3) in the greenhouse or grown in the 2008 summer nursery. After 1.5-2 weeks approximately 1 cm of leaf tissue was collected from each seedling and DNA isolation was performed in 96-well format 1.5 mL collection strip tubes. DNA extraction buffer (350 µL of extraction buffer consisting of 6.24 mM Potassium ethyl xanthaogenate (PEX), 100 mM Tris pH 7.5, 2 M NaCl, 10 mM EDTA) was added to each tube. The fresh leaf tissue was ground in a TissueLyser (Qiagen) with one 3.2 mm stainless steel bead (Spectramedix) in each tube for 4 min at 30 Hz. The orientation of the plates was reversed and ground for an additional 4 minutes. The plates were then incubated at 65°C for 20 min, cooled at -20°C for 10 min, and centrifuged in an Allegra 25R centrifuge (Beckman) at 5,800xg for 8 min to pellet debris. To precipitate the DNA, 200 µL of supernatant was transferred to a 96-well deep well plate (VWR) containing 200µL of ice-cold isopropanol. DNA was pelleted by centrifugation (6,000xg for 10 min at 4°C) and the pellet washed with 150 µL of 70% ethanol. Residual ethanol was allowed to evaporate and DNA was then resuspended in 100 µL of autoclaved, sterilized water. DNA was stored at -20°C and was heated for 10 min at 65°C prior to PCR analysis.

Optimization of Multiplexed Polymerase Chain Reaction (PCR)

PCR primers were first designed for *sbe1* and *sbe2a* to allow for the multiplexing of primers that isolated the genotype for the mutant and wildtype alleles of each gene within a single PCR reaction. For *sbe1,* primers 1A4 (5'-TGG GAT GCG ATT TGC CTG GGA AAT ACA G-3'), 1A7978 (5'-CTG GAC AGG GAA CAA GGA AC-3') and 1A7400Mu (5'- CCG CTT TTT GTC TAT AAT GAC AAT TAT CTC CAC GG-3') were designed using the Primer3 primer design algorithm (17). A second set of *sbe1* primers and a set of *sbe2a* primers were designed using muPlex (16), an algorithm for designing primers specifically for use in multiplexed reactions. For *sbe1,* 1A6950F (5'- TCC CTT TTG CCT GTG GT-3'), 1A7814R (5'-GGA ACT GCT CCT GTA CAT ACA AAC T-3') and 1AMU2 (5'- CTA TAA TGA CAA TTA TTT CCA CGG TA-3') were multiplexed in a single reaction. Primers 1A6950F and 1A7814R amplify the wildtype *Sbe1* allele (approximately 100bp) and primers 1A6905F and 1AMU2 amplify the mutant *sbe1-Mu* allele (approximately 500bp). For *sbe2a*, 2A4904F (5'-CCT GGA TCC TGA GTG GTT C-3'), 2A4976R (5'-TGG TGG TGG GAT AAC TCG-3'), and 2A4466Mu (5'-TGG CAA TTA TCT CGT CGT G-3') were designed using the muPlex algorithm (Appendix 2). The wildtype *Sbe2a* allele PCR product was approximately 900 bp and the *sbe2a-Mu* allele was approximately 500 bp (Appendix 2). Each primer set was optimized for primer concentration and additives including BSA, DMSO, and KCl. PCR cycling programs were optimized for annealing time, annealing temperature, and extension time. The *sbe2a* multiplexing reaction was successfully optimized using a recipe of 1X PCR buffer (20 mM Tris HCl pH 8.4, 50 mM KCl), 1.5 mM MgCl, 0.2 mM dNTPs, 0.25 μM of each primer, 0.01 M KCl, 0.8 mg/mL BSA, 0.8 units of Taq, 2 μL of template, and 5% glycerol. Each of the primers was subjected to a touchdown program, with a lowering of annealing temperature per cycle, to assess

if that increased specificity in multiplexing. The reactions were amplified on a C1000 Thermal Cycler (BioRad) using a touchdown program of 94C for 3 min, 10 cycles of 94°C for 30 sec, 64°C for 45 sec decreasing -0.8°C per cycle and 72°C for 1:15, 25 cycles of 94°C for 30 sec, 55°C for 45 sec and 72°C for 1:15 followed by a final extension at 72°C for 10 min. Even with rigorous optimization, we were unable to successfully multiplex the *sbe1* reaction and the wildtype and mutant alleles were genotyped in separate reactions as described below.

Polymerase Chain Reaction (PCR) Genotyping for *sbe1* and *ae*

Seedlings segregating for the *sbe1-Mu* allele were genotyped as described in Blauth et al. (2). Briefly, the wildtype *Sbe1* allele (approximately 100 bp) was amplified with primers 1A4 (5'-TGG GAT GCG ATT TGC CTG GGA AAT ACA G-3') and 1A5 (5'-CTC TGG AAG CTT TGA CGT CGA TGC TC-3') and the mutant *sbe1-Mu* allele (approximately 500 bp) was amplified with primers 1A4 and Mu9242 (5'-AGA GAA GCC AAC GCC WCG CCT CYA T-3') in two separate PCR reactions. This was done with a standard recipe supplemented with 2 mM

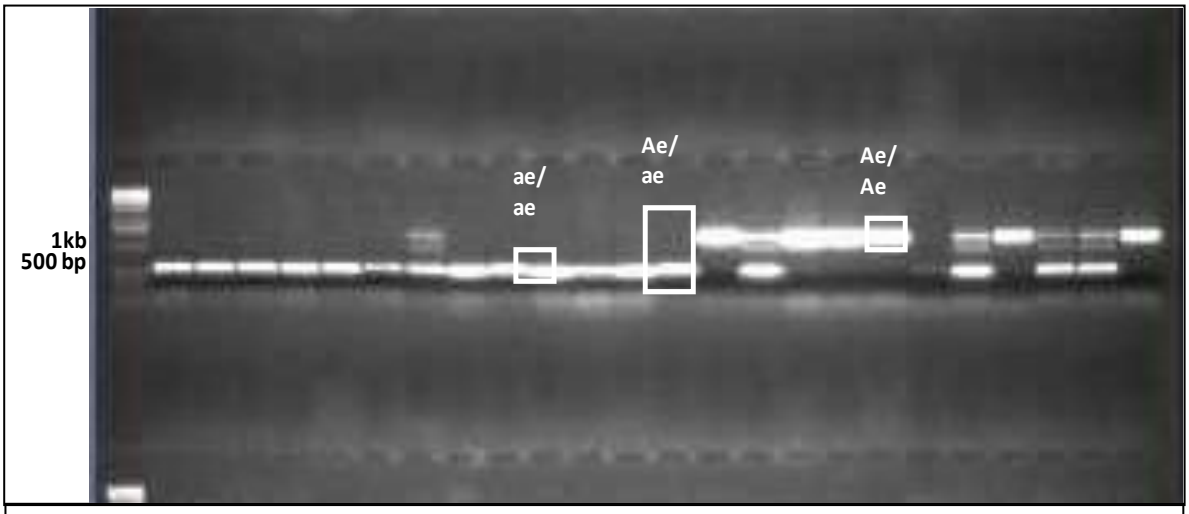

Figure 4: *Ae* PCR
Ae PCR, although not multiplexed, allows for the visualization of all three possible genotypes in one reaction due a to deletion in mutant allele.

MgCl, 0.8 mg/mL BSA, 0.8 units of Taq and 5% Glycerol. *Sbe1* gene products were amplified using the same touchdown profile described above. Wildtype *Ae* (approximately 1.4 kb) and the *ae* mutant allele (approximately 530 bp) were genotyped in a single PCR reaction using primers ae7675R (5' AGT GCT CTT GGA TTG CCA TT 3') and ae6279F (5' TAC ACC CCC TTT GGA TCC TT 3') using a temperature profile of 95°C for 3 min, 34 cycles of 95°C for 30 sec, 55°C for 45 sec, and 72°C for 1:30 min and a final extension of 72°C for 10 min. PCR reactions contained 1.5 mM MgCl and 5% glycerol. The genotyping reaction for *Ae* genotypes for both wildtype and mutant alleles in a single reaction. This is successful because the mutant allele contains a deletion, which the primers flank. Therefore, depending on the alleles present, products of different sizes result (Figure 4).

The *Ae* primer set did not require multiplexing as was necessary for the *Sbe2a* primers (Figure 4). The *ae* mutant allele contains an 882 bp deletion and the genotyping primers flank this deletion such that the *Ae* allele yields a ~1.4 kb product and the *ae* allele yields a ~530-bp product. Therefore, depending on the genotype of the plant, PCR products of different sizes result; only the 1.4 kb product for homozygous wildtype plants, both the 1.4 kb and 530 bp products for heterozygous plants and only the 530 bp fragment for homozygous mutant plants (*ae/ae*).

Gel Electrophoresis and DNA Sequencing

DNA that was amplified using the above PCR procedures was fractionated by electrophoresis on a 1.0% agarose gel, stained with ethidium bromide and visualized by digital imaging with UV transillumination (32). PCR products to be sequenced were amplified in larger quantities, run on large wells on a 1.0% agarose gel and purified from gel slices using the

QiaQuick Gel Extraction kit (Qiagen) according to manufacturer's instructions. Purified PCR product was then sent to the Genomics Core Facility at Penn State University for sequencing. The results were analyzed through comparison of the PCR chromatograph with known genomic sequences using Vector NTI software on a Dell PC computer.

Statistical Analysis

The χ^2 test for goodness of fit compared the observed rate of allele transmission to the expected rate that is predicted by Mendelian genetics. The χ^2 test for heterogeneity tested if there were differences in genotype frequencies among progeny originating from separate seed packs. Statistical analysis for the *in vitro* and *in vivo* pollen tubes experiments was performed using a one-tail T-test with two samples assuming unequal variances. The p-value that was used to test statistical significance was 0.05 for all statistical tests.

Pollen Tube *In Vitro* Analysis

Mature pollen was collected at ~11 AM from wildtype, *ae* single mutant and *sbe2a-Mu; ae* double mutant plants grown either in the 2008 genetic nursery or in the greenhouse. Pollen was germinated on solid pollen germination media (PGM; 20% sucrose, 20 mM $CaCl_2$, 0.001% H_3BO_3, 0.1 mM KH_2PO_4, 12% PEG6000) according to Schreiber *et al.* that had varying concentrations of sucrose or sorbitol (18). Concentrations of sucrose were varied from 0-4%. Ultimately, the media that showed the greatest difference between mutant and wildtype pollen tubes contained 4% sucrose, 4 mM $CaCl_2$, 0.0002% H_3BO_3, 0.02 mM KH_2PO_4, 2.4% PEG6000. After pollen was sprinkled on a plate of germination medium, pollen tube growth was observed every 15 minutes under an Olympus Szx 12 microscope with Fluorescence Attachment Szx

RFL3 (Figure 8A). Pollen tube growth was stopped by addition of 80% ethanol to each plate. Digital pictures were taken on 10X power using visible light. Pollen tube lengths were measured using ImageJ 1.37v software (39).

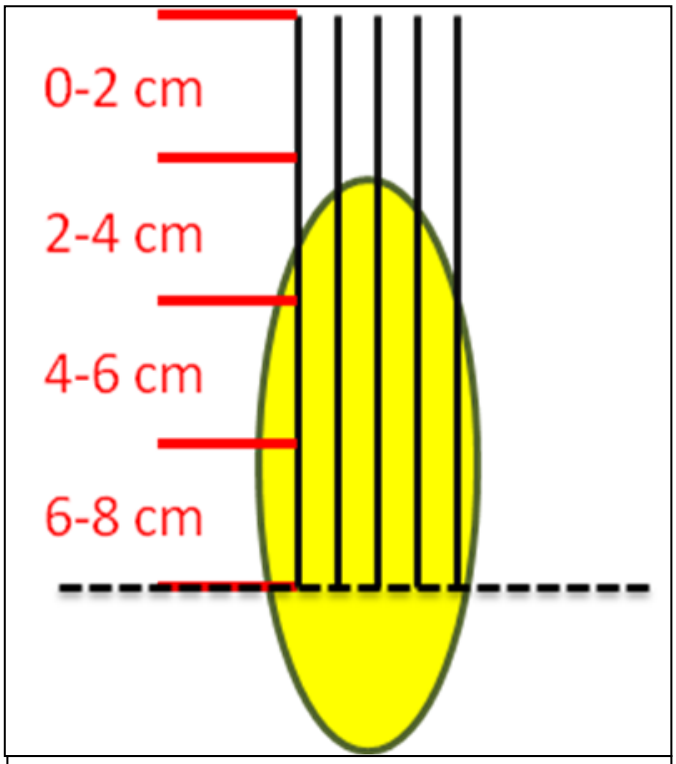

Figure 5: Silk Sectioning
Method of sectioning silks along the ear length. The yellow oval represents the ear and the black lines represent the silks. Silks were cut into 2 cm portions and each section was processed separately to examine the pollen tube growth. The dotted line represents where the ear was sliced. Only silks originating above the dotted line were sampled. The red lines delineate the cut segments.

Pollen Tube *In Vivo* Analysis

Wildtype plants were pollinated with pollen either from *ae* single or *sbe2a-Mu; ae* double mutants. After 2 and 10 hours, silks were harvested and cut into 2 cm pieces starting from the most exterior portion of the silk (0-2 cm, 2-4 cm, 4-6 cm, 6-8 cm) and placed in 5 mL vials (Figure 5). Silks were processed and pollen tubes visualized by a protocol modified from Martin (14) and Valdivia *et al.*(19). The silks were fixed in FAA (1 formalin: 8 80% ethanol: 1 acetic acid) at room temperature overnight. They were then soaked in 100% ethanol for 10 minutes and stored in 75% ethanol. When ready to be examined, the silks were hydrated through a series of ethanol dilutions: 15 minutes in each of 75%, 50% and 30% ethanol followed by 15 minutes in water. The silks were then treated with 8 N NaOH for 45 minutes. To remove residual sodium hydroxide, the silks were rinsed three times with water, each for one hour. A 0.1% aniline blue solution in 0.1 N K_3PO_4 was then added to the silks to stain the pollen tubes. The silks were examined, five silks per slide, under UV light on a compound microscope (Olympus Szx 12 with Fluorescence Attachment Szx RFL3). For each silk the total number of pollen tubes and the number extending through the segment were recorded (Appendix 1). Due to the possible error caused by the merging of tubes with vascular tissue and the subsequent difficulty in distinguishing between pollen tubes and vasculature, the number of pollen tubes germinating were then counted.

Results

Transmission of *sbe2a* and *ae* Alleles

Previously, it was established that the *sbe2a-Mu; ae* double mutant is recovered at very low rates (~6%) from a selfed *Sbe2a/sbe2a-Mu; ae/ae* heterozygote. In that selfed cross, either or both the male and female gametes, which are haploid, could be double mutant and could be the cause of the low *sbe2a-Mu; ae* transmission rate. To test if double mutant male gametes have altered transmission rates in the absence of double mutant female gametes, pollen from *Sbe2a/sbe2a-Mu; ae/ae* plants were crossed to either wildtype or *Sbe2a/Sbe2a; ae/ae* single mutant females. The goal was to determine the rate that the *sbe2a-Mu* and *ae* alleles are transmitted together in an outcross to wildtype or *ae* single mutant females. This cross directly tests whether there is a pollen defect in the absence of any potential defects in egg cells lacking *Sbe2a* and *Ae.* Progeny kernels were germinated, DNA was isolated from seedlings and each was genotyped to ascertain the *sbe2a* genotype using our newly developed multiplexed genotyping approach. If double mutant pollen was transmitted normally, one would expect 50% *Sbe2a/Sbe2a; ae/ae* and 50% *Sbe2a/sbe2a-Mu; ae/ae* progeny. However, when *Sbe2a/sbe2a-Mu; ae/ae* was crossed to *Sbe2a/Sbe2a; ae/ae*, in only 7.5% (19/254) of progeny was the *sbe2a-Mu* allele transmitted (Table 2). The p-value for a χ^2 goodness of fit test to an expected ratio of 1 *Sbe2a/Sbe2a; ae/ae:* 1 *Sbe2a/sbe2a-Mu; ae/ae* is 8.8846×10^{-10}. This shows that there is a highly significant difference between the transmission of the *sbe2a-mu; ae* double mutant genotype observed here compared to that predicted by Mendelian genetics. Similarly, when *Sbe2a/sbe2a-Mu; ae/ae* was crossed to *Sbe2a/Sbe2a; Ae/Ae* wildtype females, only 9% of resulting progeny contained the *sbe2a-Mu* allele (14/168; Table 3). The p-value for the χ^2goodness of fit test is 3.396×10^{-27}. Again, this is highly statistically significant, showing a

difference between the predicted transmission of the mutant allele and the experimental observations. The rates obtained when crossing the heterozygote to either a *Sbe2a; Ae* or an *Sbe2a; ae* female do not statistically differ (p-value= 0.212).

Table 2: Numbers of Plants Recovered from the Cross between *Sbe2a/Sbe2a; ae/ae x Sbe2a/sbe2a-Mu; ae/ae*

Greenhouse Row[a]	*Sbe2a/sbe2a-Mu; ae/ae*	*Sbe2a/Sbe2a; ae/ae*	Total
115	0	45	45
116	5	40	45
117	2	44	46
118	2	44	46
Field grown	10	62	72
Total[b]	19	235	254

[a]The plants labeled greenhouse row are plants that were grown during the fall season in the greenhouse. "Field grown plants" were grown in the field over the summer of 2008. These data were combined because the genotype frequencies do not significantly differ among the greenhouse rows and field samples (p-value for a χ^2 test for heterogeneity is 0.88, when row 115 was removed due to heterogeneity with other rows).
[b]The p-value for χ^2 goodness of fit test to an expected ratio of 1 *Sbe2a/Sbe2a; ae/ae:* 1 *Sbe2a/sbe2a-Mu; ae/ae* is 8.8846×10^{-10}.

Table 3: Number of Plants Recovered from the Cross Between *Sbe2a/Sbe2a; Ae/Ae* x *Sbe2a/sbe2a-Mu; ae/ae*

Greenhouse Row[a]	*Sbe2a/sbe2a-Mu; Ae/ae*	*Sbe2a/Sbe2a; Ae/Ae*	Total
119	7	31	38
120	2	40	42
121	2	41	43
122	3	42	45
Total[b]	14	154	168

[a]All greenhouse rows were be combined, as genotype frequencies did not significantly differ among rows (p-value for a χ^2 test for heterogeneity is 0.673, when row 119 was removed due to heterogeneity with other rows).
[b]The p-value for the χ^2 goodness of fit test to an expected ratio of 1 *Sbe2a/Sbe2a; Ae/Ae:* 1 *Sbe2a/sbe2a-Mu; Ae/ae* is 3.396×10^{-27}.

The above data demonstrates that *sbe2a-Mu* transmission through pollen, in the absence of potential female gamete effects, is affected in an *Sbe2a/sbe2a-Mu* heterozygote in an *ae* background. To understand how *sbe2a-Mu; ae* mutant pollen is or is not affected in an *sbe2a-Mu; ae* homozygote, pollen from either an *Sbe2a/Sbe2a; ae/ae* or an *sbe2a-Mu/sbe2a-Mu; ae*/*ae* homozyogous plant was crossed to wild type *Sbe2a/Sbe2a; Ae/Ae* and single mutant *Sbe2a/Sbe2a; ae/ae* plants. Upon maturation, ear phenotypes were observed (Figure 6).

Sbe2a; ae x *Sbe2a; ae* *Sbe2a; ae* x *sbe2a-Mu; ae* *Sbe2a; Ae* x *sbe2a-Mu;ae*

Sbe2a; ae *Sbe2a; ae* *Sbe2a; ae* *sbe2a-Mu; ae* *Sbe2a; Ae* *sbe2a-Mu; ae*

Figure 6: Effects of *Sbe* Mutations on the Ear of the Plant
Images were taken of ears resulting from the indicated crosses. There is no effect of the *sbe2a* mutation on the phenotype of *ae* (wrinkled kernels) and no maternal effect.

Ears pollinated by *Sbe2a; ae* single mutant or *sbe2a-Mu; ae* double mutant pollen were very similar in phenotype. Importantly, the ears pollinated with double mutant pollen exhibit a similar number of kernels and a full seed set very similar to the ears resulting from pollination with *Sbe2a; ae* pollen. We observed no aborted kernels or "gaps" where egg cells were unsuccessfully pollinated, demonstrating that *sbe2a-Mu; ae* pollen is completely viable and can successfully pollinate when coming from a homozygous *sbe2a-Mu/sbe2a-Mu; ae/ae* plant. However, when multiple pollen genotypes are present, as in a *Sbe2a/sbe2a-Mu; ae/ae* heterozygote, *sbe2a-Mu; ae* double mutant pollen grains have a reduced frequency of successful pollination as shown in Tables 2 and 3. Together, the results suggest that the *sbe2a-Mu; ae* pollen germinates more slowly or pollen tubes grow at a slower rate than *Sbe2a; ae* or *Sbe2a; Ae* pollen because when *sbe2a-Mu; ae* double mutant pollen and *Sbe2a; ae* single mutant pollen are produced together, only 7.5% - 9% transmission results (Tables 2 and 3).

Table 4: Summary of Transmission of *sbe2a-Mu* and *ae* alleles

Cross[a]	Expected Genotype Percentage	Observed Genotype Percentage
Sbe2a/sbe2a-Mu; ae/ae selfed plant	25% double mutants	6% double mutants [b]
Sbe2a/Sbe2a; Ae/Ae x *Sbe2a/sbe2a-Mu; ae/ae*	50% containing *sbe2a-Mu*	9% containing *sbe2a-Mu*
Sbe2a/Sbe2a; Ae/Ae x *sbe2a-Mu/sbe2a-Mu; ae/ae*	Full Seed Set	Full Seed Set [b]

[a]Expected genotypes predicted from Mendelian genetics and observed genotypes obtained from and genetic analysis of plants, respectively

[b]Data that was previously obtained from experiments from Marna Yandeau- Nelson and Ryan Wolff

After determining that *sbe2a-Mu; ae* pollen is viable and can pollinate, but does not successfully pollinate at expected rates when non-double mutant pollen is present, it was essential to examine the pollen to identify its defect. Both *in vitro* and *in vivo* analyses were performed to test for differences between *Sbe2a; Ae* and *Sbe2a; ae* pollen versus *sbe2a-Mu; ae* double mutant pollen. We examined the lengths of pollen tubes both *in vitro* and *in vivo* to determine if the lower rate of double mutant recovery was due to a decreased growth rate of double mutant pollen tubes. If the double mutant pollen did not grow as long or at a competitive rate with wildtype or single mutant pollen, then the difference in *sbe2a-Mu; ae* transmission rate could be due to the inability of the *sbe2a-Mu; ae* double mutant pollen to reach the egg cell in a timely manner and compete for fertilization.

In Vitro Experiments

In vitro experiments were first used to examine the pollen in *sbe2a-Mu/sbe2a-Mu; ae/ae* double mutant and *Sbe2a/Sbe2a; ae/ae* single mutant plants. Pollen tubes were grown on varying levels of sucrose and sorbitol to determine the optimal lowest sucrose concentration on which wildtype pollen grains could germinate. Since we were examining double mutants in which two key enzymes in starch synthesis (i.e., SBEIIa and SBEIIb) were not functional, the addition of sucrose to the media could compensate for the absence of starch in the double mutant, and thereby mask any potential pollen phenotype. Therefore, it was necessary to have the lowest amount of sucrose necessary for wild type pollen to grow. Concentrations of sucrose were varied from 0-4%. At the lower concentrations of 0 and 1%, pollen grains burst and exhibited little tube growth. With the addition of more sucrose, pollen tubes germinated and grew. Therefore, it was found that 4% sucrose was optimal for pollen tube germination. Pollen tubes from various genotypes were grown on this media and were examined after incubation periods of 4 or 5 hours (Table 5). The lengths of pollen tubes in the double mutant and single mutant pollen samples were then measured and compared using Image J software (Figure 7B). In the *in vitro* experiments, the results showed a significant difference between the lengths of pollen tubes in double mutant, *sbe2a-Mu; ae*, and single mutant, *Sbe2a; ae* pollen.

Table 5: *In vitro* pollen tube experiments show a difference between pollen tube length of double mutant *sbe2a-Mu; ae* and single mutant *Sbe2a; ae* Plants After 5 hours (A) and 4 hours (B). Sizes are in micrometers.

A.

Genotype	Average Tube Length After 5 Hour Incubation
Sbe2a; ae	3.23±1.03 μm
sbe2a-Mu; ae	2.79±0.99 μm

B.

Genotype	Average Tube Length After 4 Hour Incubation
Sbe2a; ae	2.36±0.51 μm
sbe2a-Mu;ae	1.57±0.31 μm

A) Pollen tubes were significantly shorter in *sbe2a-Mu; ae* pollen (p-value= 0.0045). *Sbe2a; ae* single mutant pollen was taken from *Sbe2a-Mu; ae* double mutant pollen was taken from two biological replicates, plants 08-1006-5 (n=42 pollen grains) and 08-1011-1 (n=74 pollen grains). The single and double mutant data in A represents 116 single mutant pollen tube and 68 double mutant pollen tube measurements. Mean ± standard deviation is reported.
B) Pollen tubes were significantly shorter in *sbe2a-Mu; ae* pollen (p-value = 1.39×10^{-10}). *Sbe2a; ae* single mutant pollen was taken from plants 08-1012 and *sbe2a-Mu;ae* double mutant pollen was taken from plants 08-1013. The single and double mutant data in B represents 82 single mutant pollen tubes and 48 double mutant pollen tube measurements. Mean ± standard deviation is reported.

Panel A **Panel B**

***Sbe2a; Ae* Wildtype Pollen from 1031-3**

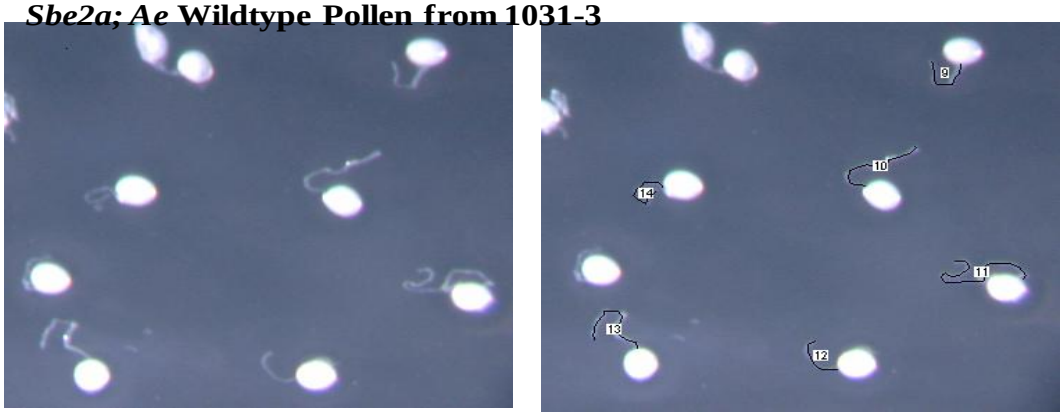

***Sbe2a; ae* Single Mutant Pollen from 1006-5**

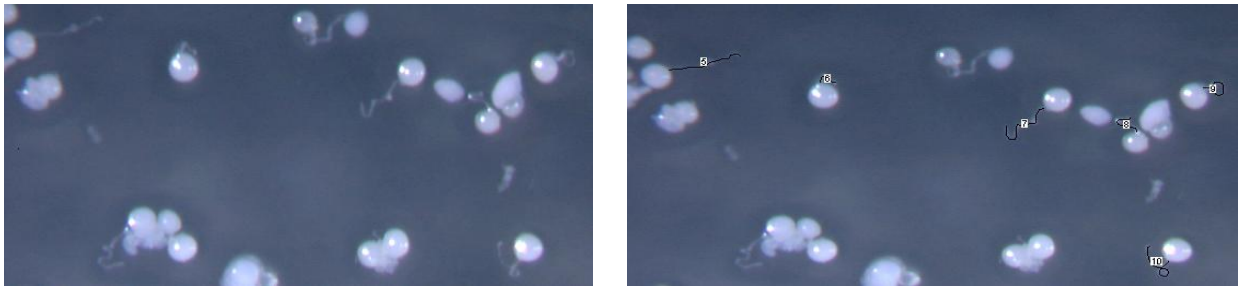

***sbe2a-Mu; ae* Double Mutant Pollen from 1013-8**

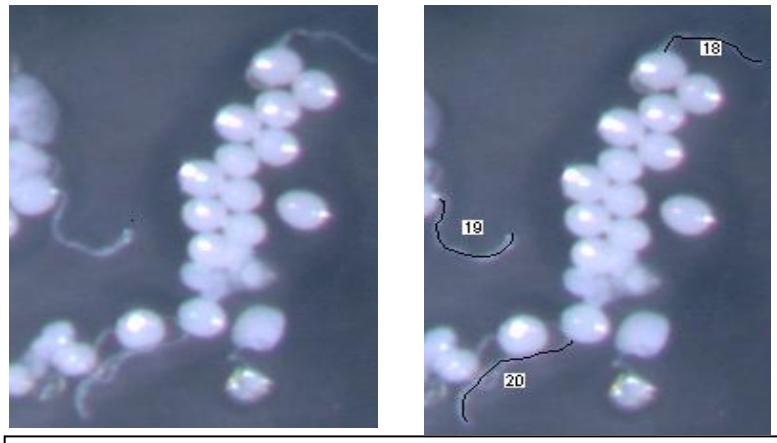

Figure 7: *In Vitro* Pollen Experiments: Pollen Grains Before and After Measuring. Pollen grains collected from *Sbe2a/Sbe2a; Ae/Ae* (wildtype), *Sbe2a/Sbe2a; ae/ae* (single mutants) and *sbe2a-Mu/sbe2a-Mu; ae/ae* (double mutants) plants were photographed 5 hours after inoculating the germination media. In Panel B, Image J was used to trace and measure the length of pollen tubes captured in Panel A.

The *in vitro* experiments showed a difference in tube length between the *Sbe2a; ae* single mutant and the *sbe2a-Mu; ae* double mutant pollen grains (Table 5). After a 5 hour incubation

period, the *sbe2a-Mu; ae* double mutant was on average 0.44 μm shorter than the *Sbe2a; ae* single mutant. After a 4 hour incubation period, the *sbe2a-Mu; ae* double mutant was on average 0.79 μm shorter than the *Sbe2a;ae* single mutant. This data suggests that the double mutant may take longer to start germinating and growing, or could be growing at a slower rate. To examine if the double mutant pollen was taking a longer time to germinate, the data was reanalyzed to determine the percentage of pollen tube germination (Table 6). The results showed that the percentage of pollen tubes germinated from *sbe2a-Mu; ae* double mutant pollen was lower and significantly different than that seen in *Sbe2a; ae* single mutant pollen for both the four hour and five hour time periods. However, there was no significant difference between the double mutant or single mutant pollen germination at the two time periods (single mutant p-value for the t-test = 0.40, double mutant p-value for the t-test = 0.15). This shows that most if not all pollen had germinated by the first time point under the conditions of this study.

Table 6: *In Vitro* Pollen Examination Shows Differing Germination Rates between Double and Single Mutant Pollen

A. Germination after 4 hours on *in vitro* germination media

Genotype	Total Pollen Granules	Pollen that Germinated	Germinated Pollen
Sbe2a; ae	130	100	77%
sbe2a-Mu; ae	134	63	47%

B. Germination after 5 hours on *in vitro* germination media

Genotype	Total Pollen Granules	Pollen that Germinated	Germinated Pollen
Sbe2a; ae	241	175	76%
sbe2a-Mu; ae	184	97	55%

A) There is a significant difference between the *Sbe2a; ae* single mutant and *sbe2a-Mu; ae* double mutant pollen tube germination (p-value of t-test = 8.75×10^{-5}). *Sbe2a; ae* single mutant pollen was taken from 82 pollen grains in row 08-1012 and *sbe2a-Mu; ae* double mutant pollen was taken from 48 pollen grains in row 08-1013.

B) There is a significant difference between the *Sbe2a; ae* single mutant and *sbe2a-Mu; ae* double mutant pollen tube germination (p-value of one-tailed t-test assuming unequal variances = 0.0006). *Sbe2a; ae* single mutant pollen was taken from *Sbe2a-Mu; ae* double mutant pollen was taken from two biological replicates, plants 08-1006-5 (n=42 pollen grains) and 08-1011-1 (n=74 pollen grains).

Since the *in vitro* experiments suggested differences in pollen tube length between the single mutant and double mutant pollen, it was necessary to further examine the pollen through *in vivo* methods, which would allow for examination of the pollen tubes growing within their natural environment, the silks.

In Vivo Examination of Pollen Tubes

In vivo experiments were used to verify the significance of the data obtained in the *in vitro* examination of pollen tubes and to visualize the pollen tube genotypes in their native environment. This experiment was designed to determine if in the natural environment, the length of pollen tubes of *sbe2a-Mu; ae* double mutants are shorter than *Sbe2a; ae* single mutants. The hypothesis was that this difference in transmission of the double mutant could be due to two reasons: 1) there could be differing growth rates between the pollen tubes of single vs. double mutant pollen grains, which would result in different pollen tube lengths in *Sbe2a; ae* pollen as compared to *sbe2a-Mu; ae* pollen, or 2) there could be differing pollen germination rates resulting in fewer *sbe2a-Mu; ae* pollen tubes for fertilization.

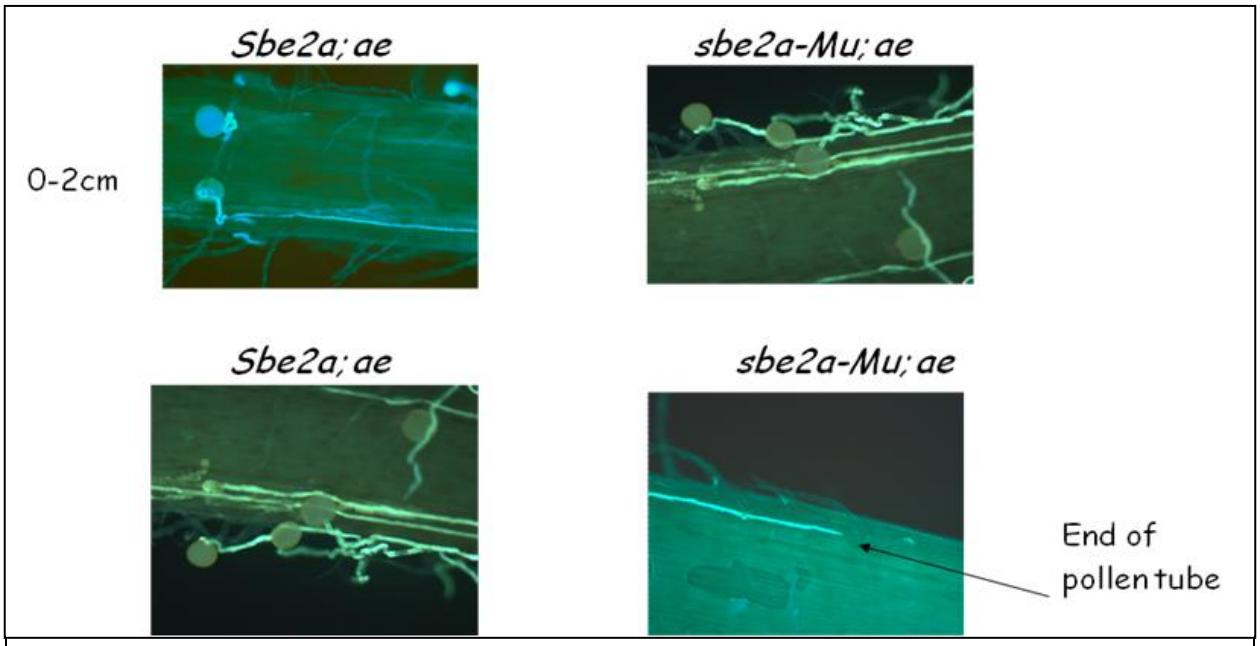

Figure 8: *Sbe2a; ae* Single Mutant and *sbe2a-Mu; ae* Double Mutant Pollen Growth within Wildtype Silks.

Silk segments were dyed with aniline blue and pollen tubes from *Sbe2a; ae* single mutant and *sbe2a-Mu; ae* double mutant genotypes were visualized under a UV microscope.

Single *ae* mutant and *sbe2a-Mu; ae* double mutant homozygous pollen was collected either from the field or greenhouse and used to pollinate wildtype females. After a specific number of hours, ten or two, pollinated ears were harvested from the plants and silks were cut into

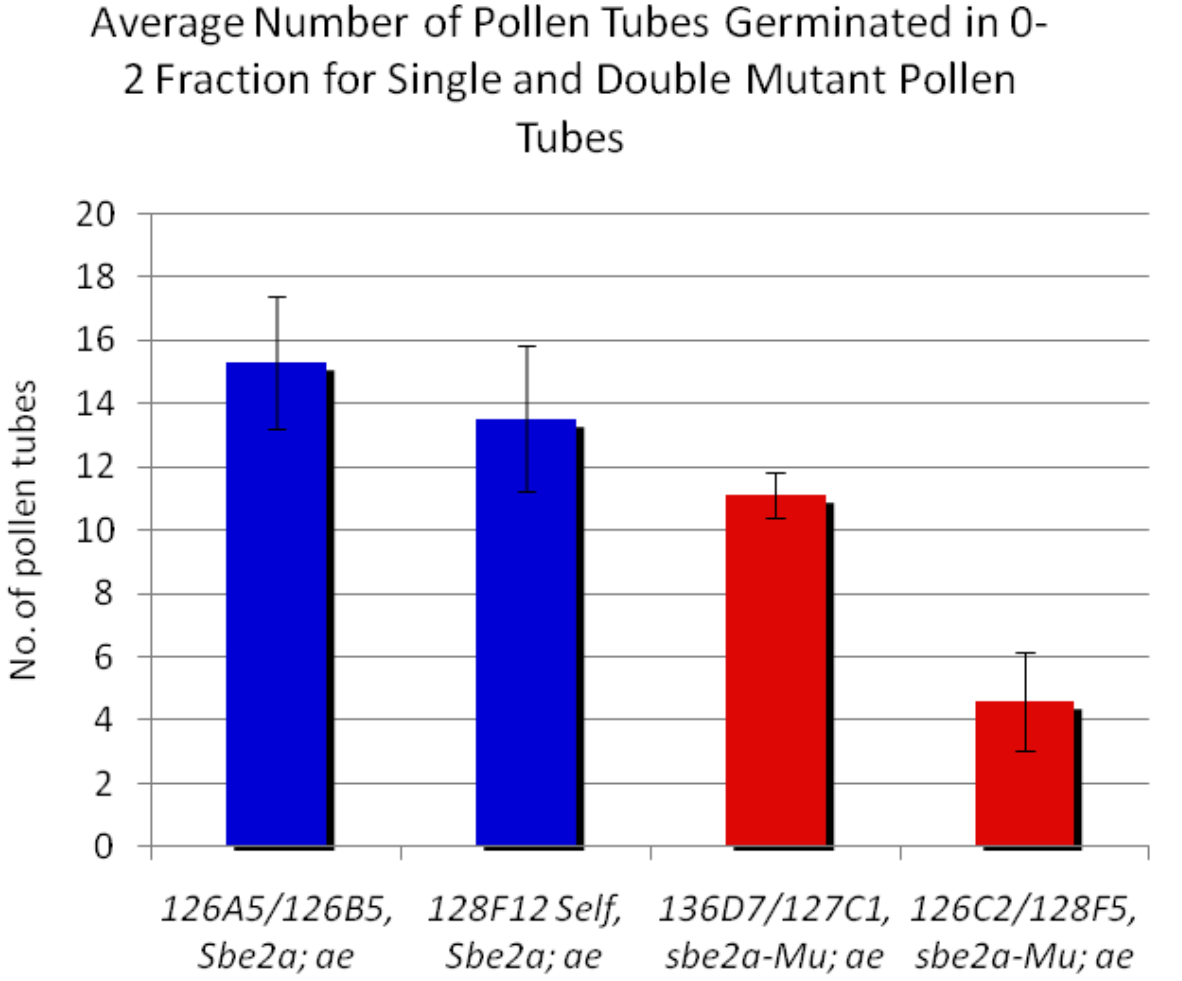

Figure 9: A New Approach to *In Vivo* Pollen Techniques: An Examination and Comparison of the Number of *sbe2a-Mu; ae* Double Mutant and *Sbe2a; ae* Single Mutant Pollen Tubes Germinated in the Wildtype 0-2 cm Silk Portion After Two Hours. The number of tubes germinated were counted, displaying a difference between *Sbe2a; ae* single mutant and *sbe2a-Mu; ae* double mutant pollen. *sbe2a-Mu; ae* double mutant pollen has significantly less germination than *Sbe2a; ae* single mutant pollen (P-value < 0.000241). N=30 silks for all genotypes. Error bars represent the standard error of the mean.

manageable 2-cm portions that could be easily viewed on a microscope slide. Silks were treated with aniline blue, a dye that reacts with the callose in pollen tubes, allowing visualization of the pollen tubes within the silks (Figure 8).

Silks were collected after just two hours and the total numbers of tubes germinated were counted. In multiple samples, a difference could be seen in the number of pollen tubes germinated in the 0-2 cm section of the silks between single mutant and double mutant genotypes (Figures 9). This data suggests that there is a different number of pollen tubes which germinate between the single and the double mutant pollen. The experiments therefore show that both *in vivo* and *in vitro* results suggest a difference in pollen tube growth and/or germination of the double mutant pollen and *Sbe2a; ae* single mutant pollen, due either to differing lengths or rates the pollen is growing or different germination rates. This suggests that wildtype pollen could be on average faster to reach and fertilize the egg, resulting in the skewed transmission genetics we observed. The single mutant pollen could possibly grow more rapidly, and therefore extend through more sections of the silk, whereas the double mutant pollen ends in earlier sections. Alternatively, the germination data from 0-2 cm also shows that there are more germinated pollen tubes for the *Sbe2a; ae* single mutant and therefore the *sbe2a-Mu; ae* double mutant could possibly take longer to germinate, and never catch up to the growth of the single mutant.

Discussion

Sbe2a-Mu and *ae* Mutant Alleles were Transmitted Together in Male Gametes at an Extremely Low Rate.

By crossing the pollen of a *Sbe2a/sbe2a-Mu; ae/ae* heterozygote to *Sbe2a/Sbe2a; Ae/Ae* or *Sbe2a/Sbe2a; ae/ae* plants, we demonstrated that the *sbe2a-Mu; ae* double mutant combination was transmitted at a frequency much lower than predicted (7.5-9.0% vs. 50%, Tables 2-3). These results suggest that there is a factor that is inhibiting the transmission of the double mutant genotype. The experimental design of this cross required the transmission of both the *sbe2a-Mu* and *ae* alleles through pollen (i.e., the egg cells were either *Sbe2a; Ae* or *Sbe2a; ae*). Thus, it is clear that a lack of class II SBEs in the pollen interferes with, but does not eliminate, allele transmission. Importantly, when an *sbe2a-Mu; ae* homozygous pollen source was used to pollinate wildtype or *ae*/*ae* ears a similar number and size of seeds were produced, indicating that the double mutation is not by itself blocking pollen or seed development; in other words, the double mutant pollen can still develop, grow and fertilize egg cells, and this can result in the development of viable seed. This data suggested that the double mutant pollen either germinates more slowly or pollen tubes grow at a slower rate than the single mutant or wildtype pollen grains, but are completely viable and able to successfully pollinate if they reach their target (i.e., egg cell).

The current data supports the previously established information that the level of starch can affect the pollen tube growth (13). Datta *et al.* (13) demonstrated that pollen maturation in maize can be terminated if the starch content is low. If starch content does not reach a threshold point, the pollen collapses during the starch accumulation phase (13). Pollen maturation was not terminated in these experiments, as indicated by ears of full seedset resulting from pollination

with the *sbe2a-Mu; ae* homozygous pollen (Figure 6). However, the starch structural change caused by the *sbe2a-Mu; ae* double mutation seemed to affect the pollen tube's ability to compete with non mutant pollen and thus to transmit the genotype at the expected frequency (Tables 2 and 3). This indicates that the starch structure determined by the action of the SBE enzymes is important for pollen tube growth or germination.

To verify this hypothesis, the starch structure in wildtype and double mutant pollen would need to be examined. These experiments, however, are quite difficult because they require large amounts of starch, which in turn requires large amounts of pollen. To determine the molecular structure of the starch, high-performance size-exclusion chromatography (HPSEC) analysis could be performed. HPSEC separates molecules on the basis of size, such that smaller molecules (e.g., small glucan branches) elute more slowly than larger molecules (e.g., longer glucan chains). Native and debranched starch molecules can be run through the chromatograph to show structure. To analyze the branching structure of amylopectin, amylopectin is first debranched with isoamylases and then the resulting glucan fragments can be subjected to HPSEC. This method can measure the relative amounts of glucan fragments of specific lengths within the debranched sample and, thereby, provide information as to the lengths of glucan branches (i.e. the number of glucose monomers within a branch) within the starch (40). This can be used to compare the starch in wildtype and mutant plants, which may differ in the branching content (5).

However, information about the starch structure within *sbe2a-Mu; ae* mutant endosperm is available, and this can be used to form hypotheses about the possible structure of starch in the double mutant pollen (Huan Xia, Ph.D. thesis, PSU 2009, manuscripts pending and personal communication, 38). In the endosperm, *sbe2a-Mu* single mutant starch is not affected, however

sbe2a-Mu has profound effects on starch structure in the leaf (Table 1). Therefore, the *sbe2a-Mu* mutant could have significantly changed starch structure, or starch structure similar to wildtype. It is important to note that we have not seen aberrant allele transmission of *ae* by itself. When an *Ae/ae* plant is selfed, approximately 25% of the kernels are *ae/ae*, as expected. Therefore, the change in starch structure/content in *ae* pollen, if any, does not seem to significantly affect allele transmission. Similarly, allele transmission is not affected in a selfed *Sbe2a/sbe2a-Mu* cross. Hence, the transmission is only affected through the combination of both *ae* and *sbe2a-Mu* mutations. The starch structure in the double mutant pollen most likely has a larger amylose content and amylopectin with a longer chain length, as seen in the endosperm, in comparison to wildtype (Table 1). Since starch serves as a source of energy for pollen tube growth, this change in starch content could affect the *sbe2a-Mu; ae* double mutant's ability for germination and growth, leading to a decrease in transmission rate.

In Vitro and *In Vivo* Pollen Tube Experiments Suggest that Double Mutant Pollen Tubes Grow to Differing Lengths in Comparison with Single Mutant Pollen Tubes

In vitro experiments examined the pollen tube growth of *sbe2a-Mu; ae* double mutant pollen and *Sbe2a; ae* single mutant pollen on synthetic media. A significant difference was observed between the length of the pollen tubes extending from *sbe2a-Mu; ae* double mutant as compared to *Sbe2a; ae* single mutant pollen (p-value =0.0045), the average length of double mutant pollen tubes was approximately 0.44 μm shorter. Our *in vitro* data at two different time points (Table 5), therefore suggested that *Sbe2a; ae* single mutant pollen tubes would extend further into the silk than *sbe2a-Mu; ae* double mutant pollen tubes. Because the need to add sucrose to the synthetic media in the *in vitro* experiments could bypass a pollen grain's need for starch of a proper structure, we also examined pollen tube growth within silks. The data shows

that more pollen grains initiated pollen tubes in the *Sbe2a; ae* single mutant pollen as compared to *sbe2a-Mu; ae* double mutant grains. This suggests that the combination of the *sbe2a-Mu* and *ae* mutant alleles in a single pollen grain leads to a change in the starch composition, due to the absence of SBEIIa and SBEIIb enzymes, which prevents or somehow impedes its normal use for growth of the pollen tubes. The second method of examining the *in vitro* data, in which percentage of pollen tubes germinated was calculated, agreed with the *in vivo* studies, showing that there was a larger number of pollen tubes that germinated in the single as compared to the double mutant pollen. It is possible that the *in vivo* data could be due to a difference in the number of pollen grains that fell on each silk, affecting the number of tubes germinated. However, *in vitro* analysis of pollen at 4 and 5 hours incubation suggests that the percentage of pollen grains to germinate is decreased in double mutant pollen (Table 6). Since there was a decrease in the germination rate for double mutant pollen, it is predicted that the mutation affects the pollen germination rate. It is possible, therefore, that the *Sbe2a; ae* single mutant pollen and the *sbe2a-Mu; ae* double mutant pollen grow at similar rates, the double mutant pollen is not able to catch up due to its decreased germination.

Future Prospects

To determine if the pollen is affected in germination or growth rate, the single and double mutant pollen grains growing within the wildtype silks could be viewed at more intervals (for example instead of just 2 hours and 10 hours, the silks from various plants could be imaged every hour in between). By counting the germinating pollen grains, as well as the tubes growing through each section, it could be determined how the pollen is affected by the double mutation. The *in vivo* studies could be further optimized to see pollen tube tips, and thereby distinguish

pollen tubes from nearby vasculature within the silks. The end of the pollen tube contains the area of rapid growth, through tip growth, with cells including two nuclei. One of these nuclei produces the pollen tube (i.e., the tube nucleus), whereas the other nucleus (i.e., the generative nucleus) produces two sperm cells (36). To better monitor tube growth, pollen tubes could be stained both with DAPI to visualize tube nuclei at the tip of the tube and with aniline blue to stain the callose within the pollen tube. *In vivo* experiments could also be done in which the ratio of the two different pollen genotypes is varied. As seen by the decreased transmission of the double mutant allele, currently single mutant pollen is more competitive than double mutant pollen. By altering the ratio of single to double mutant pollen, we could gain further evidence to support this hypothesis. Future experiments could also include further examination of germination of pollen *in vitro*. Analysis of plates at 15 minute intervals could help to provide information on the effect of germination in double mutant plants.

Summary

These experiments suggest that either, or both, the rate at which the pollen tubes grow or the germination success is affected by the double mutation. It is possible that the change in starch structure in the double mutant pollen results in starch that is degraded more slowly than in wildtype pollen. The change in the branches of the starch structure due to the *sbe* mutations could form starch that is less easily degraded. This would result in double mutant pollen with starch that is less readily available for pollen tube growth resulting in slower germination and growth and thus reduced competitiveness for fertilization versus wildtype pollen.

Chapter 2

Production of Mutant Recombinant SBE Proteins for Biochemical Analysis of Redox Regulation

Introduction

Redox Regulation of Enzymes Involved in Starch Biosynthesis

One of the remaining mysteries of how the SBE enzymes function in plants is whether their activities are regulated during plant growth and if so, by what mechanisms. As a start to answer this question, our lab is testing the possibility that the SBEs are regulated by the reduction-oxidation (redox) cycle found in many plant cells and known to be a major regulatory mechanism of many enzymes. Oxidation is the process whereby a molecule loses electrons, and reduction is the opposite process, in which electrons are gained. Redox regulation is a mechanism by which an enzyme's activity is regulated through oxidation and reduction. Ferredoxin, an iron-sulfur protein that mediates electron transfer, is a key component in redox regulation. Ferredoxin reduces thioredoxin, a protein that facilitates the reduction of other proteins by cysteine thiol-disulfide exchange (3). This reduction occurs during light dependent photosynthetic electron transport, via the transfer of reducing groups from ferredoxin to thioredoxin by ferredoxin: thioredoxin reductase. The reduced thioredoxin can then react with

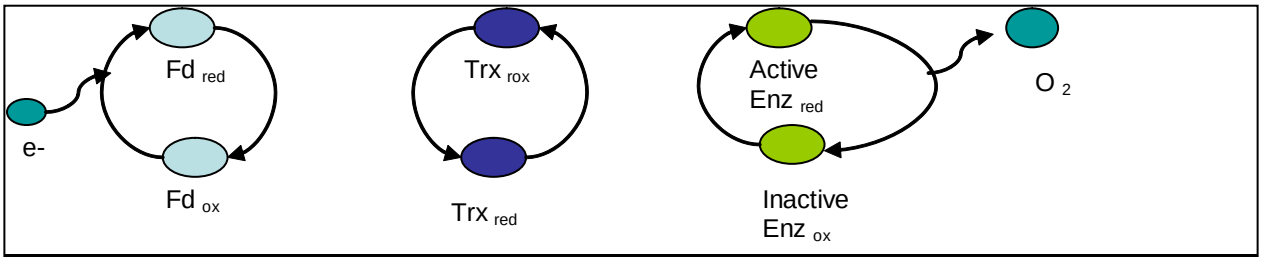

Figure 10: Ferredoxin and Thioredoxin Electron Chain Transport
The transport of electrons, as seen between ferredoxin and thioredoxin, is essential for redox regulation that occurs in starch synthesis in response to light and sugars.

and reduce various targets (3) (Figure 10). It has been suggested that this mechanism regulates starch synthesis in response to light and sugars (3).

Several proteins involved in starch synthesis have already been shown to be redox regulated (Figure 11), including ADP-glucose pyrophosphorylase (AGPase) (3). AGPase is a key regulatory enzyme of starch synthesis that catalyzes the conversion of glucose-1-phosphate and ATP to ADP-Glc and PPi, which is the first committed step in the pathway (3). In an oxidative environment, the small subunits of AGPase are linked via a disulfide bridge, and the enzyme is inactive. In the presence of light, reduced thioredoxin reduces the disulfide bridge between the small subunits, thus activating the enzyme (Figure 11). The fact that redox activates this enzyme during the day is consistent with starch synthesis occurring in the presence of light when photosynthesis occurs.

Light dependent redox regulation of starch synthesis in areas of the plant not directly associated with light (e.g., within the kernel endosperm) is thought to be possible (3). The ferredoxin: thioredoxin reductase mechanism can control starch synthesis in organs not exposed to light because during photosynthesis, carbon dioxide is converted to triose-phosphates, which

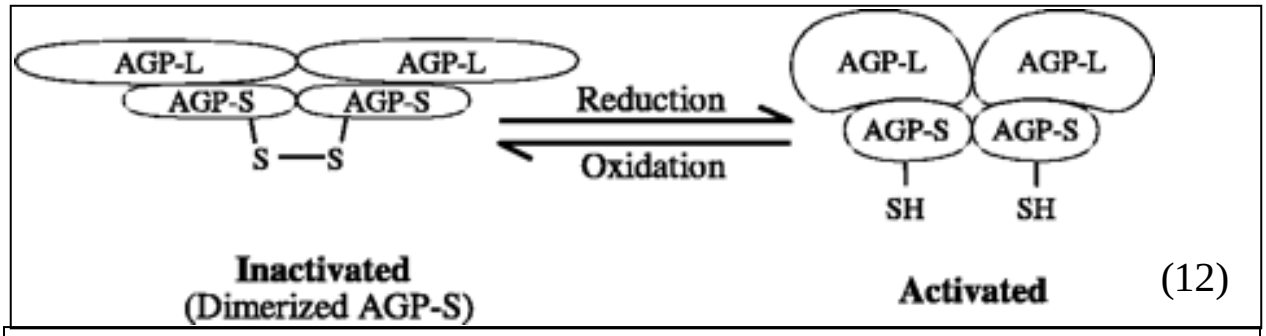

Figure 11: AGPase Redox Regulation

AGPase is a key regulatory enzyme of starch synthesis that is controlled by redox. When oxidized, the small subunits of AGPase are linked by a disulfide bridge and the enzyme is inactive. However, when AGPase is reduced the disulfide bridge is broken and the enzyme is activated to regulate the conversion of glucose-1-phosphate and ATP to ADP-Glc and PPi.

serve as a transportable signal of redox regulation. Triose-phosphate molecules accumulate during photosynthesis and are either used in the chloroplast to synthesize transient starch or are exported throughout the plant to synthesize sucrose (3). AGPase regulates starch synthesis in response to an imbalance between photosynthesis and triose-phosphate export, which correlates with changes in 3-phosphoglyceric acid to Pi ratio (3). This allows for starch synthesis to be regulated by light, even though it is not in an organ that is exposed to light.

Redox also regulates other proteins involved in starch biosynthesis and other processes. *In vitro* work has shown increased activity of maize pullulanase (ZPU1) when incubated with thioredoxin, which suggests similar post-translational redox modification in maize starch synthesis enzymes (21**)**. The major enzymes involved in *de novo* fatty acid synthesis and ammonium assimilation have also been suggested by recent research to be regulated by redox regulation (e.g., acetyl-CoA carboxylase, glutamine synthetase, and glutamine:oxoglutarate amino transferase) (3). These enzymes are controlled by similar redox mechanisms as AGPase, and can therefore provide information on the mechanism.

Chapter Rationale and Organization

As a first step in this analysis, my objective was to create mutated versions of the SBE genes, express these in *E. coli* and purify recombinant proteins for further study. These mutant proteins will be used to analyze the redox control of starch synthesis in a study outside of the scope of the work presented in my thesis. The mutations were carefully chosen due to the known importance of cysteine in redox regulation (12). The primary target of redox regulation is the sulfydryl group (RSH) on cysteine residues, which is oxidized to disulfide bonds (RSSR), sulfenic acid (RSOH), sulfinic acid (RSO_2H), or sulfonic acid (RSO_3H) (37). Cysteine is therefore regulated

by redox because it has free sulfhydryl groups in a reducing environment and disulfide bonds in an oxidizing environment. Enzymes in the Calvin cycle, ATP synthesis and NADPH export from chloroplasts are activated by the reduction of cysteine residues. It was previously determined that the regulatory site of AGPase is a cysteine residue and that multiple cysteine residues contributed to the regulation of the enzyme (12). By analyzing heterologously expressed SBEIIa and variants of this enzyme, we will provide a better understanding of the factors that regulate the production of starch in the plant. Variants of this enzyme were created by changing cysteine (Cys) residues to alanine (Ala) and by mutating multiple cysteines to alanine in a single construct.

Materials and Methods

Protein Isolation/Purification

SBEIIa Constructs

The *sbe2a* cDNA sequence coding for the mature SBEIIa protein (i.e., without the chloroplast leader sequence) had previously been transformed into the pET28a (Novagen) vector to generate the N-terminal His-tagged pMYN080118N-C4 construct. This plasmid was then used to generate six new constructs in which a single Cys residue was mutated to an Ala. The six point-mutant constructs were pMYN080505-C522A (Cys->Ala mutation at residue 522 relative to the numbering in GenBank Accession No. AAB67316), pMYN080603-C573A (Cys->Ala mutation at residue 573), pMYN080505-C577A (Cys->Ala mutation at residue 577), pMYN080505-C674A (Cys->Ala mutation at residue 674), pMYN080603-C751A (Cys->Ala mutation at residue 751), and pMYN080603-C792A (Cys->Ala mutation at residue 792). Plasmids were previously transformed into BL21 (DE3) cells for recombinant protein expression.

Preparation of Crude Protein Extracts

Liquid LB media supplemented with 30 mg/L kanamycin was inoculated with a single BL21 (DE3) colony containing one of the plasmids described above. The culture was incubated over night at 37°C with shaking at 250 rpm. Two aliquots of 5 mL were taken from the culture the next morning and used to inoculate two 2-L flasks each containing 500 mL of LB supplemented with kanamycin. The flasks were allowed to shake at 37°C at 250 rpm until the cultures reached an OD600 of ~0.6-0.8. The cultures were then induced with IPTG to a final concentration of 0.2 mM and allowed to shake at room temperature overnight. In the morning the cultures were transferred to oakridge tubes and spun at 8670 x g for 8 minutes at 4°C. The media was discarded and the pellets were briefly allowed to dry. The pellets were resuspended in 50 mL of 1X His Buffer (0.5 M NaCl, 20 mM Tris pH 8, 5 mM imidazole) and sonicated in a plastic beaker on ice for 4 cycles of 40 seconds on, 1 minute off or until the cells exhibited a color change from clear/yellowish to brown/cloudy. The broken cells were supplemented with 1 mM of the protease inhibitor PMSF. A small aliquot (the "whole cell" extract) was saved for SDS-PAGE analysis and the remainder was centrifuged for 1 hour at 4°C at 31,000 x g to pellet the cellular debris. The resulting supernatant was used for protein purification. An aliquot was saved for SDS-PAGE analysis (protein extract).

Purification of Proteins

Recombinant SBEIIa protein was purified from the crude protein extract using His-Select nickel affinity gel (Sigma). All procedures were performed at 4°C. The gel was loaded onto a 5 cm column (BioRad), cleaned with 20% ethanol and rinsed with sterilized water. The column

was charged with 10-20 column volumes of 1X charge buffer (50 mM nickel sulfate) and then equilibrated with 30 column volumes of 1X His Buffer (0.5 M NaCl, 20 mM Tris pH 8.0, 5 mM imidazole). The protein extract was run through the column and the resulting flow-through was collected and filtered through the column again. The column was washed with 30 column volumes of 1X His buffer. Contaminating proteins were eluted with 20 column volumes of 1X His Buffer supplemented with 15 mM imidazole and the SBE protein was eluted with approximately 30 mL of 1X His Buffer supplemented with 45 mM imidazole. Protein elution was monitored by testing 10 μl aliquots of eluting flow-thru with Bradford reagent (Bio-Rad). Small aliquots were taken at each wash and elution step for SDS-PAGE analysis. The 30-40 mL of eluted protein was poured into dialysis tubing (Spectrum Labs SpectraPor Dialysis Membrane: MWCO 50,000) and dialyzed overnight in 2 L of dialysis buffer (25mM Tris, pH 8.0 and 50 mM Na Cl) at 4°C.

SDS-PAGE Analysis

Aliquots taken throughout the purification procedure as described above were electrophoresed on SDS-PAGE gels with a 7% acrylamide, pH 8.8 running gel and a 4% acrylamide, pH 6.8 stacking gel. The gel was run on constant current of 80 mAmps for approximately 2 hours. The gel was then stained with Coomassie blue to visualize the proteins (32).

Concentration and Storage of Proteins

The dialyzed proteins were concentrated in a CentriPlus concentrator (Millipore) according to manufacturer's directions. The protein solution was split between two

concentrators to maximize speed. Aliquots of 10 mL were centrifuged for 20 minutes at 3123 x g and 4°C until the total volume was reduced to ~3.5 mL. Glycerol was added to 20% total volume and the purified protein was stored in small aliquots at -80°C.

Production of Mutant Constructs Containing Multiple Amino Acid Substitutions

QuikChange PCR (Stratagene) was used to create a mutant with multiple residues that are changed from cysteine to alanine. Primers were designed to introduce these substitutions using the QuikChange Primer Design program (Stratagene). PCR reactions consisted of a final concentration of 1X PFU Ultra Buffer, 0.2 mM dNTPs, 2.5 ng forward and reverse primers, 0.05U PFU Ultra, 6% DMSO, 1ng DNA from different mutant). The PCR conditions were: 95ºC for 30 sec; 18 cycles of 95ºC for 30 sec, 55ºC for 1 min, 68ºC for 8 min; 68ºC for 10 min; followed by a hold at 4ºC. After PCR, 20 µL was removed for analysis by gel electrophoresis and 1 µL of DpnI, a restriction enzyme that digests methylated plasmid DNA (i.e., remaining PCR template), was then added to the remaining 30 µL and incubated at 37ºC for 2 hours. A transformation was then completed in which 5 µL of DpnI- treated product was added to 25 µL of α-select chemically-competent *E. coli* cells and iced for 30 minutes. The cells were then heat shocked at 42ºC for 45 seconds and iced for 2 minutes. Cells supplemented with LB were allowed to recover for 1 hour at 37ºC (250 rpm) and then plated on LB plates supplemented with kanamycin. Resulting colonies were screened via PCR and subsequent sequencing to confirm the presence of the desired mutations.

Results

Generation of *sbe2a* Constructs Containing Multiple Cys-to-Ala Substitutions

To better understand the redox regulation of SBEIIa, mutants were created whereby cysteines in the protein, which are known to be important to redox regulation, were switched to alanine (12). Both single and multiple mutants were created in order to best understand the regulation. QuikChange PCR was repeated multiple times, selecting for different mutations in particular locations in order to create a SBE protein with multiple mutations of cysteine to alanine (Table 7). A single mutant was first made and the construct was confirmed. This confirmed construct was then used as template for creation of a double mutant, where mutagenesis was used to add a substitution at a second Cys site. The sequence of the double mutant was confirmed, and this was used as a template for the creation of the triple mutant, and so on, until reaching a mutant with five mutations. A quadruple mutant was produced containing the mutations of C674-573-522-751A. The C577A mutation was difficult to obtain because the primers designed for the 573 residue also contained the mutation located at position 577. Primers therefore were redesigned in order to create a mutant with all six mutations of cysteine to alanine located at 522, 573, 577, 674, 751, and 792. A SBE protein was created with five mutations of C573-674-522-751-792A, and the remaining mutation at 577 could be added by adjusting the primers. This multiple mutant is important to be able to study the effect of redox regulation on SBE, as previously described. The mutants containing multiple residue substitutions will allow to study SBE, *in vitro*, and aid in identification of the two important cysteine residues for SBE activation.

Table 7: SBEIIa Constructs

Plasmid	Position of Cys to Ala Substitution[a]
pMYN080505-C522A	Amino acid 522
pMYN080603-C573A	Amino acid 573
pMYN080505-C577A	Amino acid 577
pMYN080505-C674A	Amino acid 674
pMYN080603-C751A	Amino acid 751
pMYN080603-C792A	Amino acid 792
pMYN081114-1	Amino acids 573 and 674
pMYN081105-1	Amino acids 577 and 674
pMYN081117-3	Amino acids 522, 577 and 674
pMYN081121-3	Amino acids 522, 573, 674 and 751
pMYN081125-1	Amino acids 522, 573, 674, 751, and 792

[a]Amino acid position is relative to GenBank Accession AAB67316.

Purification of Single Mutant SBE Proteins

The His – Select nickel affinity gel column was used to purify the SBE proteins with the various mutations of cysteine to alanine. Extracts were taken at various stages of the purification and subjected to SDS-PAGE analysis to track purity of the protein. At early stages of the purification, multiple bands resulted, displaying impurities in the preparation (Figures 12-17). These impurities represent other proteins that had not yet been separated out. Because the contaminating proteins do not contain His-tags, later stages of the purification remove these contaminants as can be seen by the decrease in the number of bands, showing the success of the

purification of each of the SBE proteins (Figure 12-17). The yield for these purifications was also good, approximately 20 mg/L.

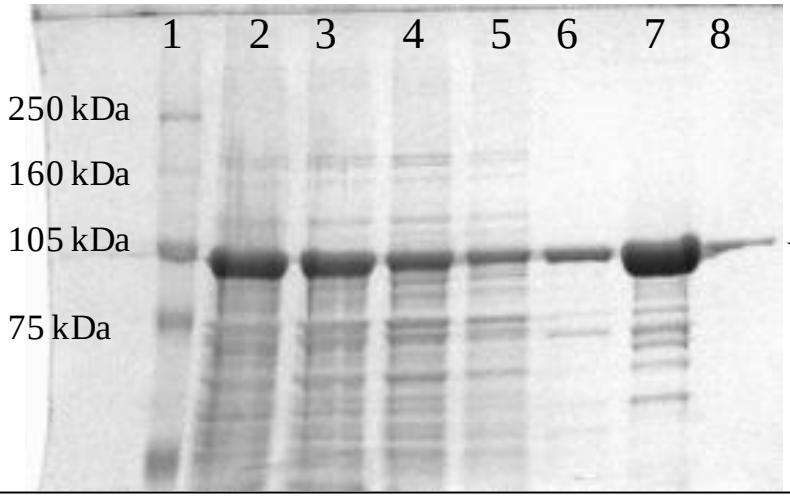

Figure 12: SBE protein C522A Coomassie Stained SDS-PAGE Gel.
Lane 1: Ladder, Lane 2: 5 µL whole cell extract, Lane 3: 5 µL cell free extract, Lane 4: 7 µL flow-thru, Lane 5: 50 µL 5 mM wash, Lane 6: 50 µL 15 mM wash, Lane 7: 50 µL 50 mM wash, Lane 8: 50 µL after dialysis. ☆ Represents the location of the SBEIIa protein.

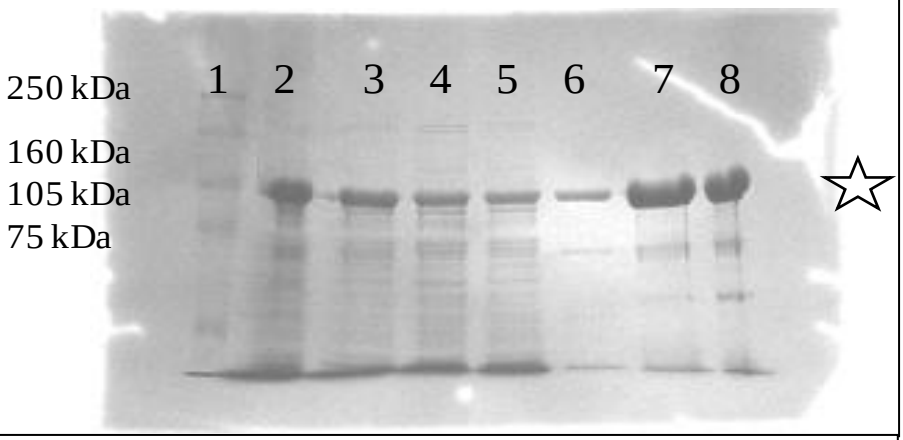

Figure 13: SBE protein C573A Coomassie Stained SDS-PAGE Gel.
Lane 1: Ladder, Lane 2: 5 µL whole cell extract, Lane 3: 5 µL cell free extract, Lane 4: 7 µL flow-thru, Lane 5: 50 µL 5 mM wash, Lane 6: 50 µL 15 mM wash, Lane 7: 50 µL 50 mM wash, Lane 8: 50 µL after dialysis. ☆ Represents the location of the SBEIIa protein.

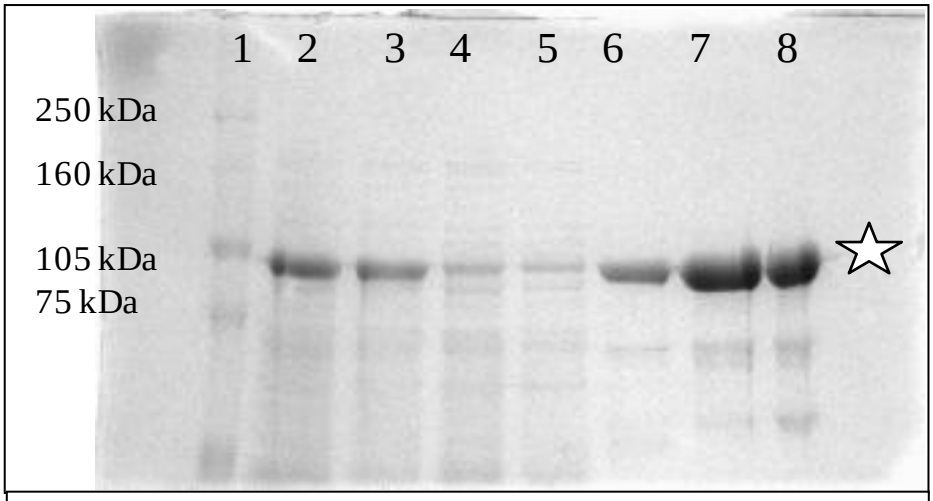

Figure 14: SBE protein C577A Coomassie Stained SDS-PAGE Gel.
Lane 1: Ladder, Lane 2: 5 µL whole cell extract, Lane 3: 5 µL cell free extract, Lane 4: 7 µL flow-thru, Lane 5: 50 µL 5 mM wash, Lane 6: 50 µL 15 mM wash, Lane 7: 50 µL 50 mM wash, Lane 8: 50 µL after dialysis. ☆ Represents the location of the SBEIIa protein.

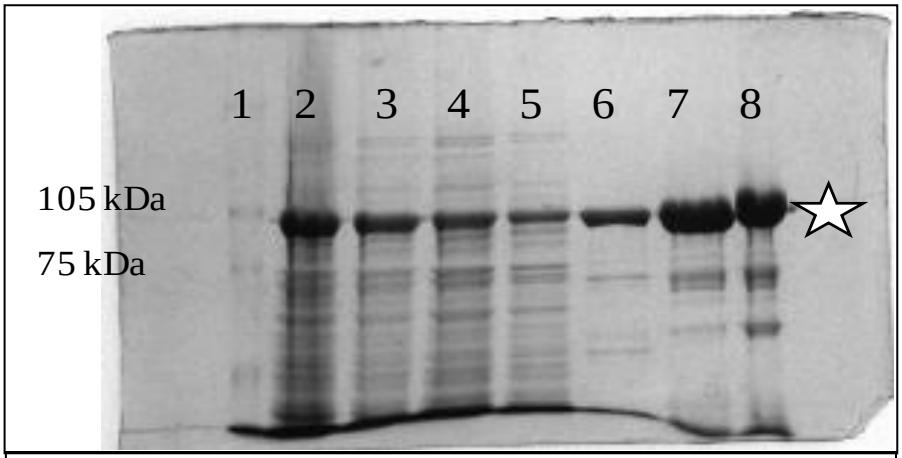

Figure 15: SBE protein C674A Coomassie Stained SDS-PAGE Gel.
Lane 1: Ladder, Lane 2: 5 µL whole cell extract, Lane 3: 5 µL cell free extract, Lane 4: 7 µL flow-thru, Lane 5: 50 µL 5 mM wash, Lane 6: 50 µL 15 mM wash, Lane 7: 50 µL 50 mM wash, Lane 8: 50 µL after dialysis. ☆ Represents the location of the SBEIIa protein.

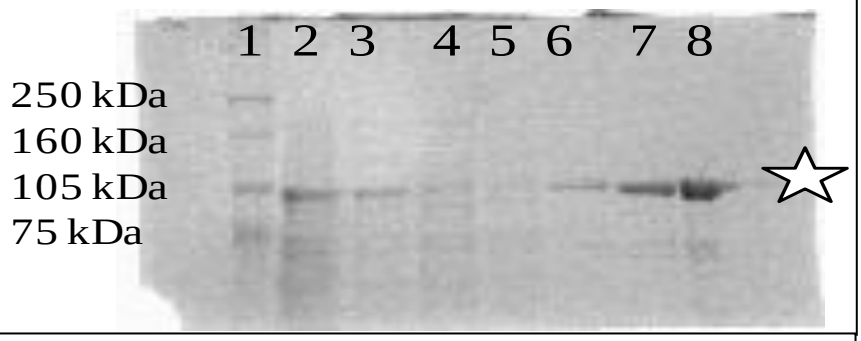

Figure 16: SBE protein C751A Coomassie Stained SDS-PAGE Gel.
Lane 1: Ladder, Lane 2: 5 µL whole cell extract, Lane 3: 5 µL cell free extract, Lane 4: 7 µL flow-thru, Lane 5: 50 µL 5 mM wash, Lane 6: 50 µL 15 mM wash, Lane 7: 50 µL 50 mM wash, Lane 8: 50 µL after dialysis. ☆ Represents the location of the SBEIIa protein.

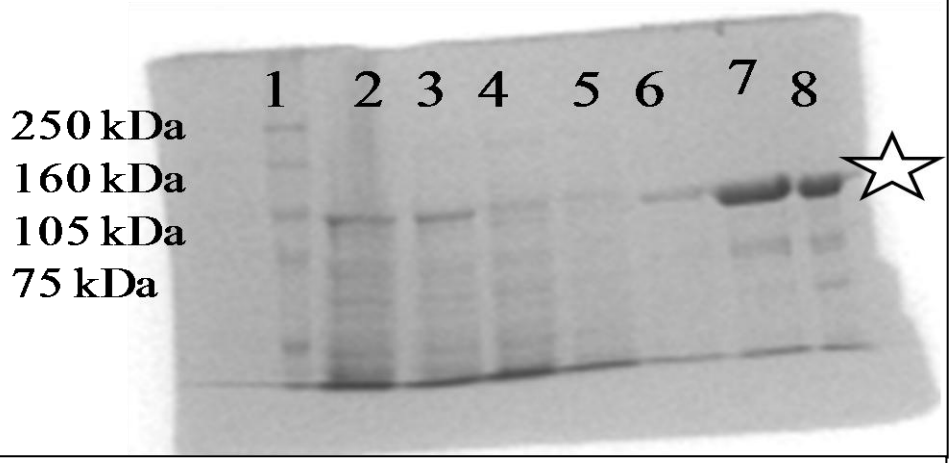

Figure 17: SBE protein C792A Coomassie Stained SDS-PAGE Gel. Lane 1: Ladder, Lane 2: 5 µL whole cell extract, Lane 3: 5 µL cell free extract, Lane 4: 7 µL flow-thru, Lane 5: 50 µL 5 mM wash, Lane 6: 50 µL 15 mM wash, Lane 7: 50 µL 50 mM wash, Lane 8: 50 µL after dialysis. ☆ Represents the location of the SBEIIa protein.

Discussion

His-Select Nickel Affinity Gel Column Successfully Purified SBE Mutants

We hypothesize that redox could regulate SBE's role in starch formation in maize. The successful purification of the various SBE mutants allows for their further use in studies surrounding the possibility of redox regulation. The SBE mutant proteins were purified to examine if removing cysteine residue(s) from the protein affects the activity of SBE in reducing or oxidizing environments, similar to redox regulation. Cysteine is an important residue for the redox regulation of many enzymes, including AGPase (12). Like AGPase, SBEIIa has cysteine residues that could be important in redox regulation. SBEIIa has six cysteine residues in the mature protein, two of which we propose have free sulfhydrl groups in the active state. We hypothesize that like AGPase, when SBE is in oxidized form, it is inactive, and the sulfur groups in the cysteine residues form disulfide bonds. We also suggest that when SBE is in a reducing

environment, the cysteines are no longer connected by a disulfide bond and instead have free sulfhydryl groups, and are therefore active. However, it is not known which two of these six cysteine groups interact, if any. The proteins were therefore purified in order to study, *in vitro*, the effect of redox regulation on the mutants, specifically aiming to find out which cysteine residues are necessary, if any, for activation. It was essential for the proteins to be purified in order to be sure there are no other proteins that may interfere with the results of the redox studies. Wildtype SBEIIa has increased activity when the protein is reduced *in vitro*. By measuring the activity of the SBEIIa mutants and comparing them to wildtype, one could determine which of the six cysteine residues are important for regulation of SBEIIa. If the mutant is no longer responsive to a change in redox environment, it suggests that the residue mutated, Cys, is key in redox regulation. Further research concerning the SBE proteins and their regulation was started, however I was not a part of it.

Appendix 1

In Vivo Pollen Analysis: Method of Counting Pollen Tube Extension, Ending, and Total Number

In Vivo Original Method Results

The following section includes the first method that was used to examine the pollen tubes *in vivo*. Initially, a method counting the number of tubes extending through each section of silk, ending in each section, and the total number of pollen tubes for each section was employed. This method was replaced by examining the number of tubes germinating, due to possible error that resulted, as described below. We predicted that the new method, which can be found in Chapter 1, was superior due to the number of tubes germinated being easier to count because the tubes should not have grown very long in two hours, reducing the number of tubes that had merged with the vascular tissue. The pollen tubes can be seen growing out from pollen grains and extending through the silks, allowing for the ability to count them (Figure 8).

First, the numbers of tubes extending through each section were counted. These tubes could be seen both entering and exiting the 2 cm section of silk. Next, the number of tubes that were ending in each section was counted. These tubes could be seen entering the silk portion, however they stopped within the section (Figure 8, bottom right panel). Finally, the total number of pollen tubes was counted for each section. By analyzing both the extension of growth as well as the ending of growth within multiple sections, we hoped to observe a difference between the wild type and mutant pollen tubes as was observed in the *in vitro* experiments (Figure 8). We hypothesized that the double mutant *sbe2a-Mu; ae* pollen tubes would end in earlier silk portions or have fewer numbers of pollen tubes that germinated due to possible effects of starch mutation within pollen.

In the double mutant silks, a reduced number of pollen tubes were observed as compared to the single mutant. There is a significant difference between the number of tubes in each of the silk segments pollinated by *Sbe2a; ae* single mutant pollen vs. *sbe2a-Mu; ae* double mutant pollen (Figure 18).

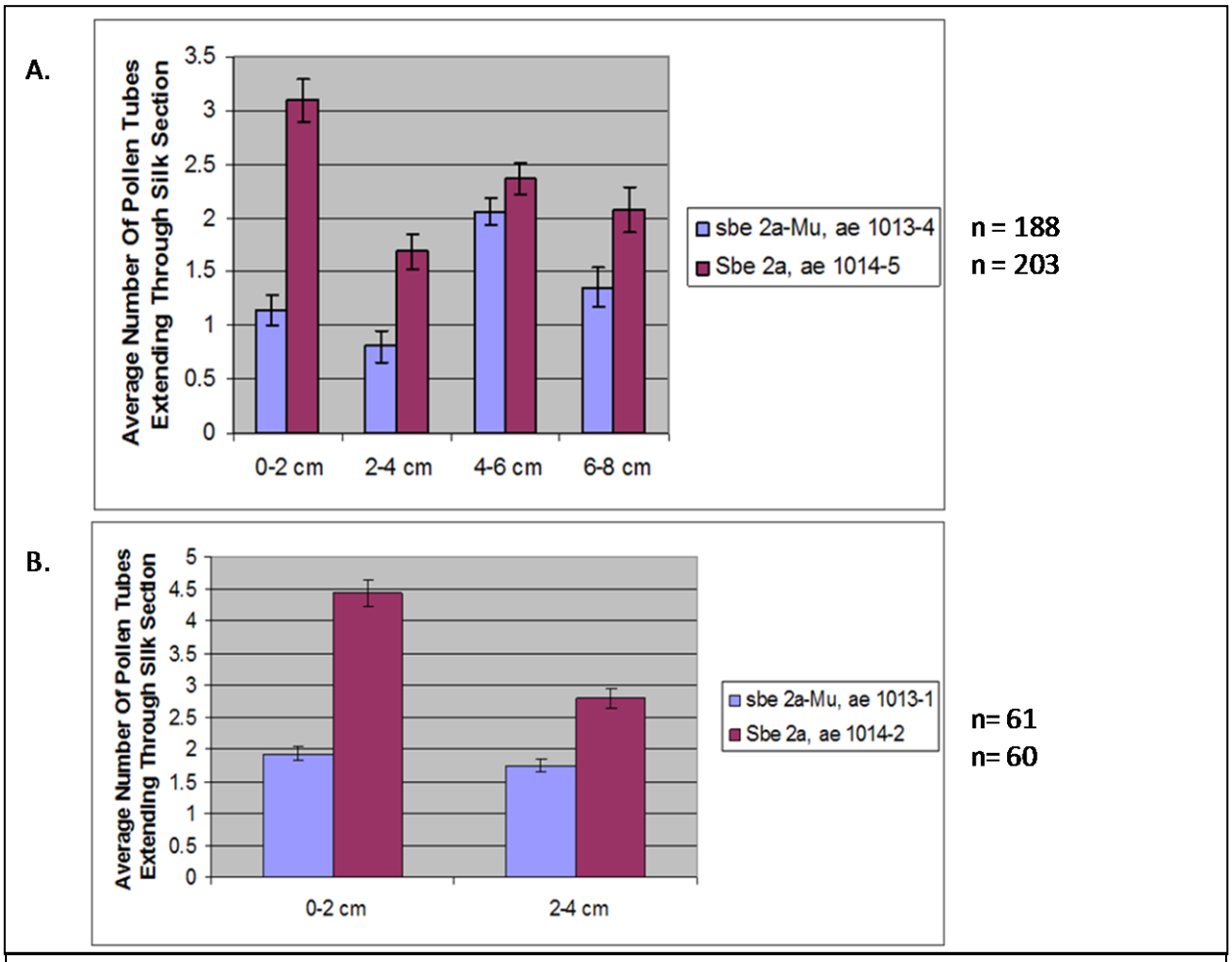

Figure 18: Differences in Single Mutant *Sbe2a; ae* and Double Mutant *sbe2a-Mu; ae* Pollen Tube Extension Through Sequential Sections of Wildtype Silks.

The number of tubes that extended through each section of silk was counted. Figure A and B represent two different biological replicates.

A. The p-value was 2.50×10^{-12} for 0-2cm section, 5.94×10^{-5} for 2-4cm section, 0.0557 for 4-6 cm section, 0.0056 for 6-8 cm section between the *Sbe2a; ae* and *sbe2a-Mu; ae* pollen genotypes. The number of silk segments analyzed (n) is shown for each genotype. Error bars represent the standard error of the mean.

B. The p-value was 6.35×10^{-15} for the 0-2cm section and 9.83×10^{-7} for the 2-4 cm section between the *Sbe2a; ae* and *sbe2a-Mu; ae* pollen genotypes. The number of silk segments analyzed (n) is shown for each genotype. Error bars represent the standard error of the mean.

As hypothesized, in every section of silk, it appeared that there were more *Sbe2a; ae* single mutant pollen tubes extending through wildtype silks than there were *sbe2a-Mu; ae* double mutant pollen tubes, displaying a difference between the growth of single and double mutant pollen tubes within the wildtype silks (Figure 18). The data suggests that the pollen tubes are growing at differing rates, with the double mutant pollen tubes extending into fewer of the longer segments of the silk. This suggests that perhaps the *Sbe2a; ae* single mutant pollen tubes are beating the *sbe2a-Mu; ae* double mutant pollen tubes to the egg cells. This would disrupt the transmission of the *sbe2a-Mu; ae* double mutant allele that is predicted by Mendelian genetics.

However, the results are likely skewed due to the fact that aniline blue, the dye used to stain the callose in pollen tubes, also stains the vasculature within silks. Because pollen tubes often grow toward and then along the vascular tissue within the silks, it was hard to distinguish between pollen tubes and vasculature. This was particularly true in the segments of silk after the 0-2 cm silk (i.e., 2-4 cm, 4-6 cm, etc.), where one could not easily trace tube extension from its origination point (i.e., the pollen grain). This could have resulted in miscounting of the tubes due to the inability to determine the difference between vasculature tissue and pollen tube growth, resulting in error in the data obtained.

In the experiments described in this appendix, we measured the number of tubes that extended through the 0-2 cm section and the number of tubes that ended in this section. This method focused on the ends of the tubes, instead of the germination in the beginning of the pollen tubes. The number of tubes germinated in the 0-2 cm section, however, could be determined because it was equal to the sum of the two previous statistics. It was determined that due to the convergence of the tubes with the vascular tissue (Chapter 1), it would be important to look at the pollen tube germination (after 2 hours). By looking at the tubes germinated in 0-2 cm

only, the data from the first experiment could be compared to the new method of obtaining data (Chapter 1). The data collected from silks in contact with pollen for 8 hours, which is included in this section, was also reanalyzed by looking at only the 0-2 cm segment of the silks (Figure 19). This figure correlates to the new method of analysis that can be seen used in Chapter 1. The new method of analysis allowed for the examination of whether germination was affected by the *sbe2a-Mu; ae* mutation. Examination of *in vitro* pollen from 4 and 5 hours incubation displayed that the germination percentage of double mutant pollen was lower than that of single mutant pollen (see Chapter 1).

The two methods of the *in vivo* experiments therefore examined the difference between single mutant and double mutant pollen in a wildtype silk in two ways, through examining the number of pollen tubes extending and ending in each section as well as through observing the number of pollen tubes germinating in the first section (Chapter 1). The first method, included in this appendix, suggested that the pollen tubes of single mutant and double mutant pollen grow at different rates. The second method, found in Chapter 1, showed that there was a different number of pollen tubes that germinated in the single versus double mutant pollen. To verify these results in the future, an *in vitro* pollen germination test examining the pollen every fifteen minutes could complement this data.

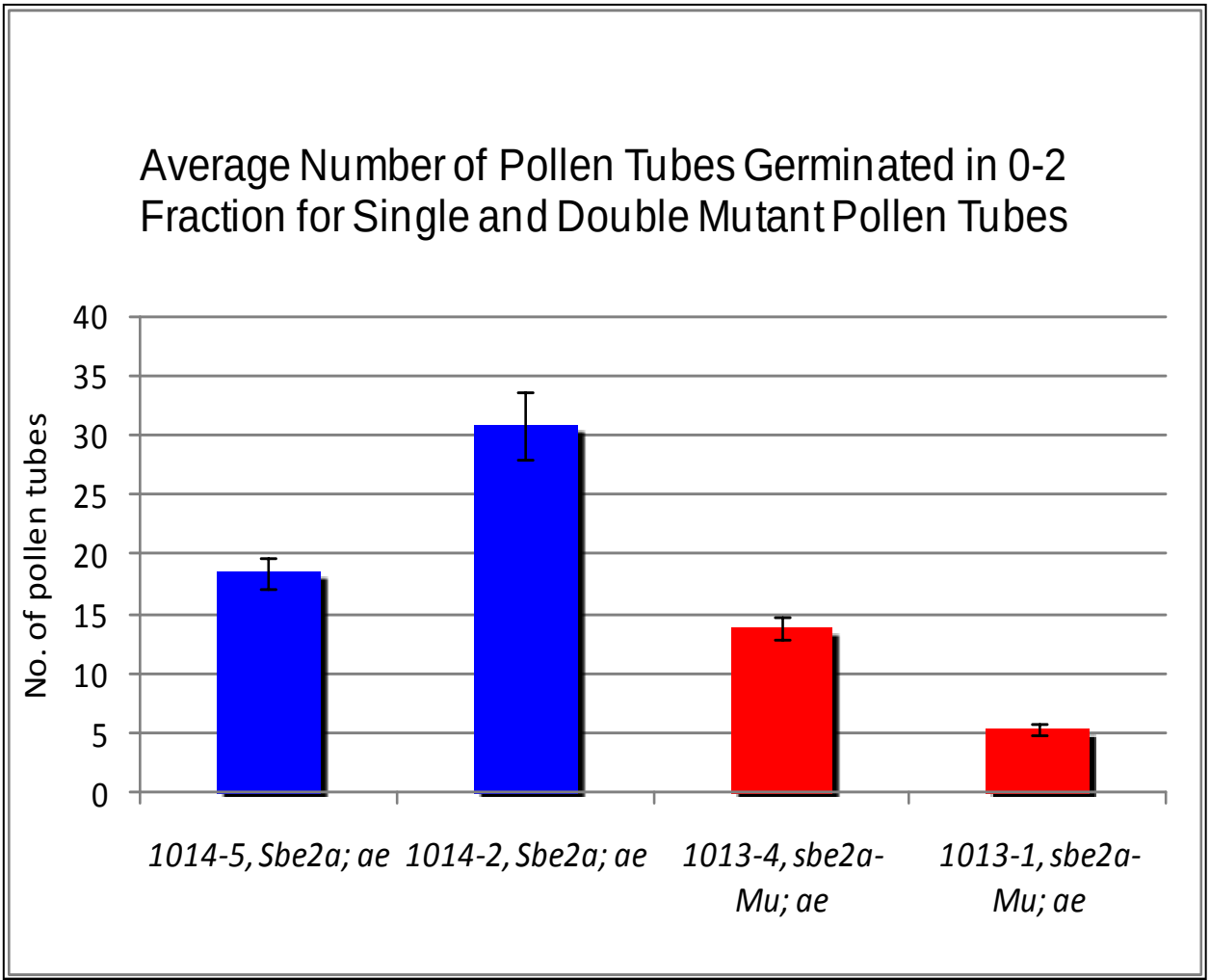

Figure 19: New Approach Applied to Old Data Obtained from *In Vivo* Techniques: Comparing the Number of Tubes Germinated for *Sbe2a; ae* Single Mutant and *sbe2a-Mu; ae* Double Mutant Pollen in Wildtype Silks.
The blue columns represent two *Sbe2a; ae* biological replicates (1014-5, n=50 silks; 1014-2, n=30 silks) and the red columns represent two *sbe2a-Mu; ae* biological replicates (1013-4, n=62 silks; 1013-1, n=30 silks). Error bars represent the standard error of the mean,
[a] *sbe2a-Mu; ae* double mutant pollen has significantly less average germination than *Sbe2a; ae* single mutant pollen (P-value < 1.22×10^{-11}).

Appendix 2

Multiplex PCR Genotyping Results and Discussion

Development of a Multiplexed PCR Approach for Genotyping *sbe2a* Alleles.

PCR was used to determine the *sbe2a* and *ae* genotypes of the different plants. Previously the *sbe2a* genotype of plants was determined by running two separate PCR reactions: primers 2A2 and 2A32 were used to amplify the wildtype *Sbe2a* allele, while primers 2A2 and Mu9242 were used to amplify the mutant *sbe2a-Mu* allele. If a plant were positive for the mutant allele

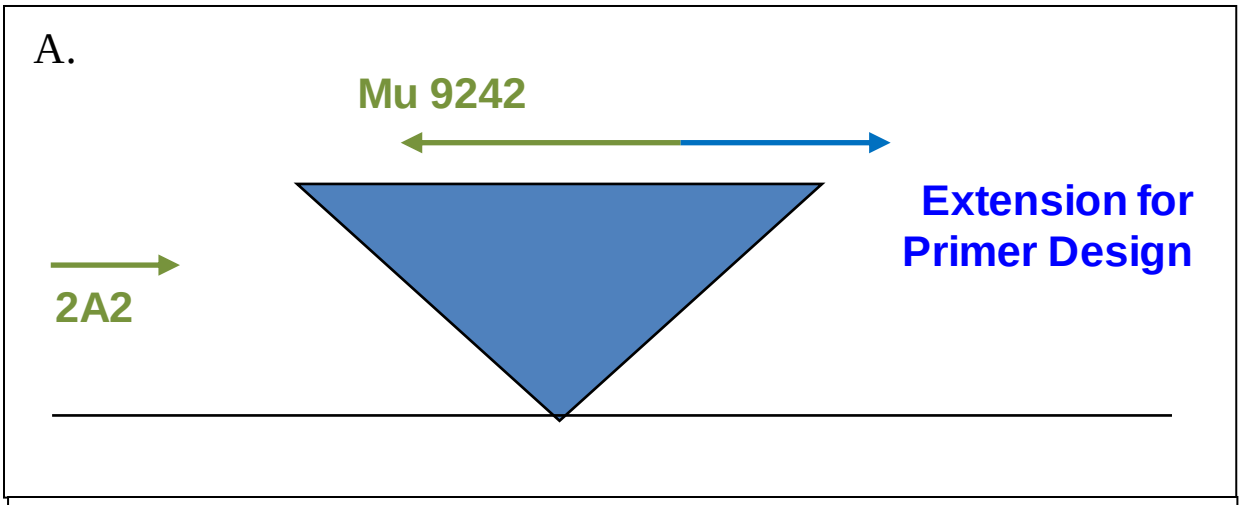

B. >2A2 PCR, Reverse- Complement

AGAGAAGCCAACGCCTCGCCTCCATTTCGTCGAATCCGCTTCTCTCTTCGTCCATAA**TGGCAATTATCTC**
GTCGTGGACACTCAACCTGAAGAACTACAGGTTCGATTGTCCCCTTCTGTGCCTCCATGGTACAAATGTC
CAAATGTCTGATGAAATCAAGTTTGGGTTTCAGCCTTTGCACTTTCATATCAGGCATTGTGCAAAGCCTC
GTGAATTGTTGGTTAGGGCACCGTGCTGGTTCTTGGGCTACTGACATTGTTAGCTTGTGATCCCACCTAC
ACCTAGCAAGAAGATCACTAAGGAATACACCATTGGTTATTTCTGTTGTTCTACACAAAACTTATCTATT
TCTTTGCTGTAGATACCTGAAGCAGAACTGACTGTGGAGAAGACATCCTCCTCACCAACTCAAACAACAT
CAGCAGTGGCTGAAGCAAGCTCAGGAGTTGAGGCTGAGGAGAGGCCTGAGCTCTCAGAAGTGATTGGAGT
TGGAGGTACTGGTGGAACCAAAATTGATGGTGCAGGCATCAAAGCCAAAGCACCACTCGTGGAGGAGAAA
CCACGAGTTATCCCACCACCAGGAGATGGCCAACGAATATA

Figure 20: Primer Design For Multiplexing of *sbe2a-Mu* PCR
A. Layout of the *sbe2a*-Mu allele and the design of the new multiplexed primer's location. The PCR product from 2A2/9242 was sequenced to produce the results in B. B. The sequence obtained from 2A2/Mu9242 PCR. The purple text is the *Mu* sequence. The green text represents the *sbe2a* genomic sequence. The bolded, larger text is the sequence representing primer 2A4466Mu, which is primarily specific to the *Mu* insertion but has six nucleotides specific to the *sbe2a* gene.

reaction and negative for the wildtype reaction, the plant would be deemed an *sbe2a-Mu* homozygote. Because large numbers of PCR were planned for the experiments detailed in this thesis, we developed a multiplexed genotyping approach to conserve reagents and time and to yield a product in each reaction indicating the full genotype of the plant at the *Sbe2a* locus.

The multiplexing approach required two gene-specific primers and a single primer that would anneal to the *Mu* insertion and also had homology to the *sbe2a* gene sequence directly flanking the insertion. This insertion site-specific primer would allow us to screen for a mutant product instead of the absence of the product when identifying the *sbe2a-Mu* allele. To design a primer specific to the insertion site, the mutant allele was amplified from *sbe2a-Mu* homozygous DNA using primers 2A2 and Mu9242 and the PCR product was sequenced. The resulting sequence extended from the "right" terminal inverted repeat of the *Mu* insertion into the genic sequence 3' of the insertion site. This sequence was used to design a primer with homology to the very 3' end of the *Mu* insertion with the three 3' bases of the primer extending into the *sbe2a* genic

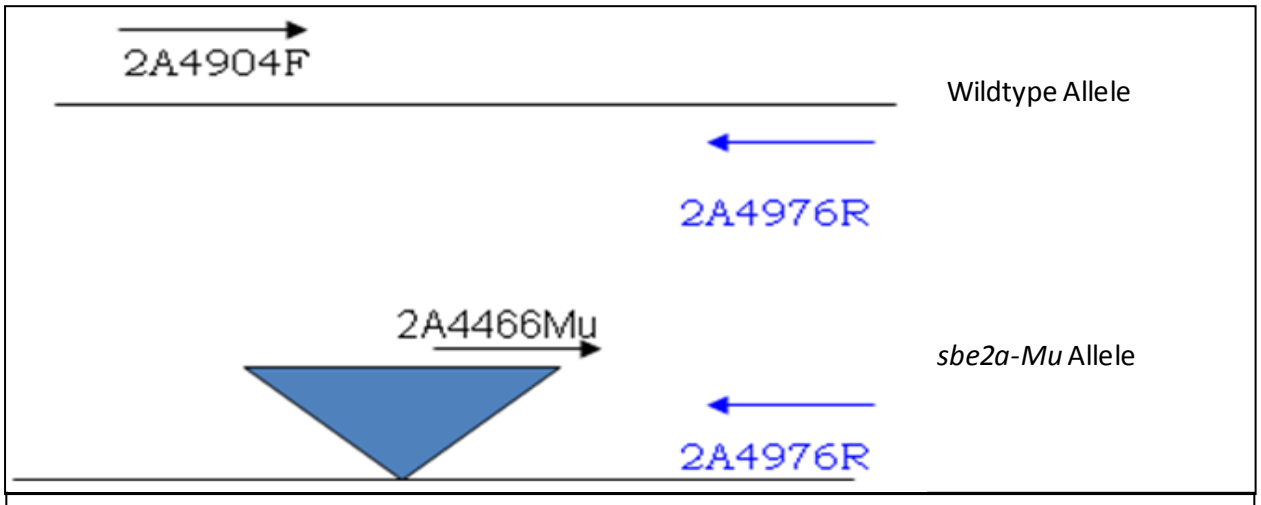

Figure 21: *sbe2a* PCR Multiplexing. Primers 2A2904F and 2A2976R amplified the wildtype allele (*Sbe2a*) and produces a 900 bp product. Primers 2A466Mu and 2A4976R amplified a 500 bp product from the *sbe2a-Mu* allele.

sequence (Figure 20).

The primers were designed (2A4904F, 2A4976R, and 2A4466Mu) to combine genotyping reactions into one single PCR run. As depicted in Figure 21, *sbe2a*-specific primer 2A4905F pairs with gene-specific primer 2A4976R to amplify a product of 900 bp in the *Sbe2a* wildtype allele. Primer 2A4976R can also pair with the *sbe2a-Mu* insertion site-specific 2A4466Mu primer to yield a product of 500 bp from the *sbe2a-Mu* mutant allele. By including these three primers in a single reaction, one PCR reaction can result in bands for both the wildtype and the mutant alleles, allowing for identification of the genotype from a single lane (Figure 22). Multiplexing of these primers required careful optimization with a specific PCR touchdown profile and well as additional additives including KCl and BSA (see Methods).

The wildtype and mutant alleles yield 900 bp and ~500 bp products, respectively (Figure 22). A single 900 bp band indicates that the genotype is homozygous wildtype. Both the 900 and 500 bp products in a single lane indicate that the genotype for that plant is *Sbe2a/sbe2a-Mu*. One 500 base pair band indicates that the genotype is homozygous mutant.

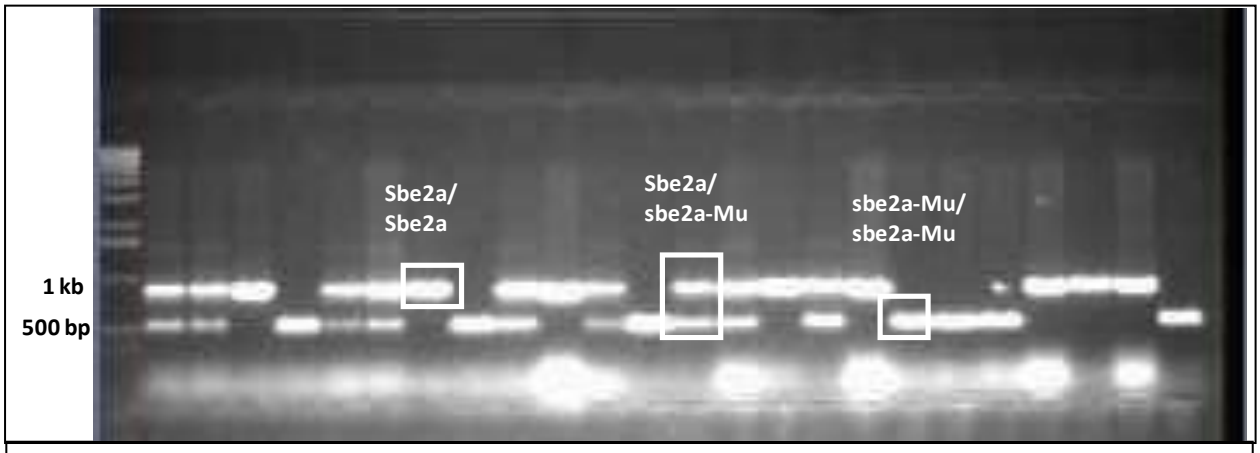

Figure 22: *Sbe2a* Multiplexed PCR
Multiplexed PCR for *Sbe2a* displaying homozygous mutant, homozygous wildtype, and heterozygous plants through the use of one reaction and three primers.

***Sbe2a* and *sbe2a-Mu* Alleles Were More Efficiently Genotyped by Implementing a Multiplexing Method.**

Previously, the *sbe2a* genotype of plants was determined by running two separate PCR reactions using primers 2A2 and 2A32 to amplify the wildtype *Sbe2a* allele and primers 2A2 and Mu9242 to amplify the mutant *sbe2a-Mu* allele. However, to more efficiently genotype the plants, a method was developed so that one reaction, in comparison to two, could be used to determine the genotype. An advantage to this method over our old method is that every reaction should have a product (i.e., a co-dominant marker). Since the multiplex primers tested for the presence of a mutation, they were able to easily identify a problem if there was no band present.

The multiplexing of the PCR reaction allowed for identification of the genotype from a single lane (Figure 22). This multiplexing is important because it allows for the conservation of both time and reactants required and results in much easier genotyping of the plants. Further use of multiplexing for the *sbe1* gene could also reduce the amount of work required. Although we were unsuccessful at multiplexing this reaction, careful optimization of the PCR reagents, including $MgCl_2$, KCl, DMSO, and BSA, and the use of a designed PCR touchdown profile could make this a viable option.

List of Works Cited

(1) James MG, Denyer K, Myers AM. Starch Synthesis in the Cereal Endosperm. *Plant Biology*. 2003;6: 215-22.

(2) Blauth SL., Kim K, Klucinec J, Shannon JC, Thompson D, Guiltinan M. Identification of *Mutator* Insertional Mutants of Starch-Branching Enzyme 1 *(sbe1)* in *Zea mays* L. *Plant Molecular Biology*. 2002; 48: 287-97.

(3) Geigenberger P, Kolbe A, Tiessen A. Redox Regulation of Carbon Storage and Partitioning in Response to Light and Sugars. *Journal of Experimental Botany*. 2005; 56: 1469-1479.

(4) Datta R, Chamusco KC, Chourey PS. Starch Biosynthesis during Pollen Maturation is Associated with Altered Patterns of Gene Expression in Maize. *Plant Physiology*. 2002; 130: 1645-1656.

(5) Yao Y, Thompson DB, Guiltinan MJ. Maize Starch-Branching Enzyme Isoforms and Amylopectin Structure. In the Absence of Starch-Branching Enzyme IIb, the Further Absence of Starch-Branching Enzyme Ia Leads to Increased Branching. *Plant Physiology*. 2004; 136: 3515-3523.

(6) Boyer C., Preiss J. Multiple forms of (1,4)-α-D-glucan, (1,4)-α-d-Glucan-6-Glycosyl Transferase from Developing *Zea mays* L. Kernels. *Carbohydrate Res*. 1978; 61:321-334.

(7) Dinges JR, Colleoni C, James MG, Myers AM. Mutational Analysis of the Pullulanase-Type Debranching Enzyme in Maize Indicates Multiple Functions in Starch Metabolism. *Plant Cell*. 2003; 15: 666-680.

(8) Gao M, Fisher DK, Kim KN, Shannon JC, Guiltinan MJ. Evolutionary Conservation and Expression Patterns of Maize Starch Branching Enzyme I and IIb Genes Suggests Isoform Specialization. *Plant Mol Biology*. 1996; 30: 1223-1232

(9) Kondrad A., Banze M, Follmann H. Mitochondria of Plant Leaves Contain Two Thioredoxins. Completion of the Thioredoxin Profile of Higher Plants. *Journal of Plant Physiology*. 1996; 129: 314-321.

(10) Wilsen K, Hepler P. Sperm Delivery in Flowering Plants: The Control of Pollen Tube Growth. *Bioscience*. 2007; 57: 835-844.

(11) Nashilevitz S, Melamed-Bussado C, Aharoni A, Kossmann J, Wolf S, Levy A. The *legwd* Mutant Uncovers the Role of Starch Phosphorylation in Pollen Development and Germination in Tomato. *The Plant Journal*. 2009; 57: 1-13.

(12) Tetlow I, Morell M, Emes M. Recent Developments in Understanding the Regulation of Starch Metabolism in Higher Plants. *Journal of Experimental Botany*. 2004; 55: 2131-2145.

(13) Datta R, Chamusco K, Chourey P. Starch Biosynthesis during Pollen Maturation Is Associated with Altered Patterns of Gene Expression in Maize. *Plant Physiology*. 2002; 103: 1645-1656.

(14) Martin FW. Staining and Observing Pollen Tubes in the Style by Means of Fluorescence. *Stain Technol*. 1958; 34: 125-128.

(15) Blauth SL., Kyung-Nam K, Klucinec J, Shannon JC, Thompson D, Guiltinan MJ. Identification of *Mutator* Insertional Mutants of Starch-Branching Enzyme 1 *(sbe1)* in *Zea mays* L. *Plant Molecular Biology*. 2002; 48: 287-97.

(16) Rachlin J, Ding CM, Cantor C, Kasif S. MuPlex: Multi-Objective Multiplex PCR Assay Design. *Nucleic Acids Research*. 2005; 33:W544-7.

(17) Rozen S, Skaletsky H. *P*rimer*3 on th*e WWW for General uUsers and for Biologist Programmers. *In: Krawetz S, Misener S (eds) Bioinformatics Methods and Protocols: Methods in Molecular Biology*. Humana Press, Totowa, NJ. 2000: 365-386.
(18) Schreiber DN, Dresselhaus T. In Vitro Pollen Germination and Transient Transformation of *Zea mays* and Other Plant Species. *Plant Mol Biol Rep*. 2003; 21: 31-41.
(19) Valdivia ER, Wu Y, Li L-C, Cosgrove DJ, Stephenson AG. A group-1 Grass Pollen Allergen Influences the Outcome of Pollen Competition in Maize. *PLoS One.* 2007: e154.
(20) Bryce W, Nelson O. Starch-Synthesizing Enzymes in the Endosperm and Pollen of Maize. *Plant Physiology*. 1979; 63: 312-317.
(21) Wu C, Colleon C, Myers AM, and James MG. Enzymatic Properties and Regulation of ZPU1, the Maize Pullulanase-Type Starch Debranching Enzyme. *Achieves of Biochemistry and Biophysics*. 2002; 406(1): 21-32.
(22) Xue S. Functional Analysis of Sucrose Synthase Genes in Maize. 2004.
(23) William L, Lemoine R, Sauer N. Sugar Transporters in Higher Plants – A Diversity of Roles and Complex Regulation. *Trends in Plant Science*. 2002; 5(7): 283-290.
(24) Zha R, Dielen V, Kinet JM, Boutry M. Cosuppression of a Plasma Membrane H+-ATPase Isoform Impairs Sucrose Translocation, Stomatal Opening, Plant Growth, and Male Fertility. *Plant Cell*. 2000; 12: 535-546.
(25) Datta R, Chourey P, Pring D, Tang H. Gene-Expression Analysis of Sucrose-Starch Metabolism During Pollen Maturation in Cytoplasmic Male-Sterile and Fertile Lines of Sorghum. *Sex Plant Reprod*. 2001; 14: 127-134.
(26) Kubo A, Fujita N, Harada K. The Starch-Debranching Enzymes Isoamylase and Pullulanase are Both Involved in Amylopectin Biosynthesis in Rice Endosperm. *Plant Physiology*. 1999; 121: 399-410.
(27) Gao M., Fisher DK, Kim KN. Independent Genetic Control of Maize Starch-Branching Enzymes IIa and IIb (Isolation and Characterization of a Sbe2a cDNA). *Plant Physiology*. 1997; 114: 69-78.
(28) Black RC, Loerch JD, McArdle FJ, Creech RG. Genetic Interactions affecting Maize Phytoglycogen and the Phytoglycogen-Forming Branching Enzyme. *Genetics*. 1966; 53(4): 661- 668.
(29) Gao M, Fisher D, Guiltinan M. Evolutionary Conservation and Expression Patterns of Maize Starch Branching Enzyme I and IIb Genes Suggests Isoform Specialization. *Plant Mol Bio*. 1996; 30: 1223-1232.
(30) Fisher D, Gao M, Guiltinan M. Two Closely Related cDNAs Encoding Starch Branching Enzyme from *Arabidopsis thaliana*. *Plant Mol Bio*. 1996; 30: 97-108.
(31) Bhattacharryya MK, Martin C, Smith A. The Importance of Starch Biosynthesis in the Wrinkled Seed Shape Character of Peas Studied by Mendel. *Plant Mol Bio*. 1993; 122: 525-531.
(32) Ausubel F, Brent R, Strauhl K. Current Protocols in Molecular Biology. John Wiley and Sons Inc. 2009; 1-5.
(33) Swinkels JJM. Composition and Properties of Commercial Native Starches. *Starch/Starke*. 1985; 37: 1-5.
(34) Blauth SL, Kim KN, Klucinec J, Shannon JC, Thompson D, Guiltinan MJ. Identification of Mutator Insertional Mutants of Starch-Branching Enzyme 1 (sbe1) in Zea mays L. *Plant Mol Biol*. 2002; 48: 287-97.

(35) Blauth SL, Yao Y, Klucinec JD, Shannon JC, Thompson DB, Guiltinan MJ. Identification of Mutator Insertional Mutants of Starch-Branching Enzyme 2a in Corn. *Plant Physiology*. 2001; 125: 1396-1405.
(36) Steer M , Steer J. Tansley Review No. 16 Pollen Tube Tip Growth. *New Phytologist*. 1989; 111 (3): 323-358.
(37) Kamata H, Hirata H. Redox Regulation of Cellular Signaling. *Cellular Signaling*. 1999; 11 (1): 1-14.
(38) Xia H. Structure and Funtion of Endosperm Starch from Maize Mutants Deficient in One or More Starch-Branching Enzyme Isoform Activities. 2009.
(39) Abramoff MD, Magelhaes PJ, Ram SJ. Image Processing with Image J. *Biophotonics International*. 2004.
(40) Yuan RC, Thompson DB, Boywer CD. Fine Structure of Amylopectin in Relation to Gelatinization and Retrogradation Behavior of Maize Starches from Three *wx*-Containing Genotypes in Two Inbred Lines. *Cereal Chemistry*. 1993; 70 (1): 81-89.

ACADEMIC VITA of Jennifer Lynne Blackman

Jennifer Lynne Blackman
8 Halter Court
Mount Laurel, NJ, 08054
Jlb5334@gmail.com

Education:

Bachelor of Science Degree in Biochemistry and Molecular Biology
Pennsylvania State University, Spring 2010
Minor in Bioengineering
Honors in Biology
Thesis Title: GENETIC AND BIOCHEMICAL ANALYSIS OF THE FUNCTIONS OF STARCH BRANCHING ENYMES IN *Zea mays.*
Thesis Supervisor: Mark Guiltinan

Related Experience:

Summer intern at Dr. Farber's Dermatology Office
Supervisor: Dr. Harold Farber
Summer 2007

Summer Volunteer at Virtua Hospital in Marlton, Emergency Department
Supervisor: Tiffany Bennett
Summer 2009

Summer Intern at The Alicia Rose Victorious Foundation
Supervisor: Gisele DiNatale
Summer 2009

Awards:

Dean's List
Phi Beta Kappa
Phi Kappa Phi
NASA's WISER Scholarship
Ruth Ott-Lewman Award

Presentations/Activities:

Global Medical Brigades
Alpha Epsilon Delta
Biochemistry and Molecular Biology Society
Undergraduate Research Exposition